# Splenic Marginal Zone B Lymphocytes Regulate Cardiac Remodeling After Acute Myocardial Infarction in Mice

Yanyi Sun, Cristina Pinto, Stéphane Camus, Vincent Duval, Paul Alayrac, Ivana Zlatanova, Xavier Loyer, Jose Vilar, Mathilde Lemitre, Angélique Levoye, et al.

▶ **To cite this version:**

Yanyi Sun, Cristina Pinto, Stéphane Camus, Vincent Duval, Paul Alayrac, et al.. Splenic Marginal Zone B Lymphocytes Regulate Cardiac Remodeling After Acute Myocardial Infarction in Mice. Journal of the American College of Cardiology, 2022, 79 (7), pp.632-647. 10.1016/j.jacc.2021.11.051 . inserm-03872700

**HAL Id: inserm-03872700**
**https://inserm.hal.science/inserm-03872700v1**

Submitted on 25 Nov 2022

**HAL** is a multi-disciplinary open access archive for the deposit and dissemination of scientific research documents, whether they are published or not. The documents may come from teaching and research institutions in France or abroad, or from public or private research centers.

L'archive ouverte pluridisciplinaire **HAL**, est destinée au dépôt et à la diffusion de documents scientifiques de niveau recherche, publiés ou non, émanant des établissements d'enseignement et de recherche français ou étrangers, des laboratoires publics ou privés.

# Splenic marginal zone B lymphocytes regulate cardiac remodeling after acute myocardial infarction in mice

Yanyi Sun, PhD[a], Cristina Pinto, PhD[a], Stéphane Camus, PhD[a], Vincent Duval, MSc[a], Paul Alayrac, MSc[a], Ivana Zlatanova, PhD[a], Xavier Loyer, PhD[a], Jose Vilar, PhD[a], Mathilde Lemitre BSc[a], Angélique Levoye, PhD[a,b], Meritxell Nus, PhD[c], Hafid Ait-Oufella MD, PhD[a], PhD, Ziad Mallat, MD, PhD[a,c], Jean-Sébastien Silvestre, PhD[a]

**Running title**: Marginal Zone B cells and Myocardial Infarction

[a]Université de Paris, PARCC, INSERM, F-75015 Paris, France
[b]Université Sorbonne Paris Nord, F-93 000 Bobigny, France
[c]Division of Cardiovascular Medicine, Cambridge University, Cambridge, United Kingdom

**Sources of Funding**: This work was supported by Fondation pour la Recherche Médicale (DEQ20160334910 to J-S.S., FDT20160435312 to I.Z.), Fondation de France (FDF 00066471 to J-S.S. and C.P.), Fédération Française de Cardiologie (to J-S.S and Y.S.) China scholarship council (CSC, No.201708310220 to Y.S.) French National Research Agency (ANR to J-S.S.) and institutional grants from Université de Paris and the French National Institute for Health and Medical Research.

**Disclosures**: The authors declare no competing financial interests.

**Corresponding author**: Jean-Sébastien Silvestre, PhD, PARCC-Inserm U970, Université de Paris, 56 Rue Leblanc, F-75015 Paris, France; e-mail: jean-sebastien.silvestre@inserm.fr; Phone: 33 1 53 98 80 60 ; Fax: 33 1 53 98 79 51

**Acknowledgments**: We are grateful to the imaging platform for small animals of Université de Paris for echocardiographic analysis.

**Abstract**
**Background.** Mature B lymphocytes alter the recovery of cardiac function after acute myocardial infarction (MI) in mice. Follicular B cells and marginal zone B (MZB) cells are spatially distinct mature B cell populations in the spleen and exert specific functional properties. miR21/Hypoxia-inducible factor (HIF)*α*-related pathways have been shown to govern B cell functions.
**Objectives.** We aimed to unravel the distinct role of MZB cells and that of endogenous activation of miR21/ HIF*α* signalling in MZB cells during post-ischemic injury.
**Methods.** Acute MI was induced by permanent ligation of the left anterior descending coronary artery in mice. Cardiac function and remodeling were assessed using echocardiography and immunohistochemistry. To determine the specific role of MZB cells, we used mice with B cell lineage–specific conditional deletion of Notch signaling, which leads to selection deficiency of MZB cells. To evaluate the role of HIF-1α isoform, we generated mice with MZB cell lineage specific conditional deletion of *Hif1a*.
**Results.** Acute MI prompted miR21-dependent increase of HIF-1α, particularly in splenic MZB cells. MZB cell deficiency and MZB cell-specific deletion of *miR21* or *Hif1a* improved cardiac function after acute MI. miR21/HIF-1α signaling in MZB cells was required for Toll-like receptor dependent expression of the monocyte chemo-attractant protein CCL7, leading to increased mobilization of inflammatory monocytes to the ischemic myocardium and to adverse post-ischemic cardiac remodeling.
**Conclusions.** This work reveals a novel function for miR21/HIF-1α pathway in splenic MZB cells with potential major implications for the modulation of cardiac function after acute MI.

**Condensed Abstract:** Splenic marginal zone B cells are instrumental in the regulation of cardiac function and remodeling after acute myocardial infarction. miR21/HIF-1*α* signaling adjusts the ability of marginal zone B cells to modulate CCL7 secretion and to subsequently impact inflammatory monocyte-dependent cardiac remodeling after injury.

**Keywords:** Myocardial Infarction, B Lymphocytes, microRNA 21, Hypoxia-inducible factor

**Abbreviations and Acronyms:**
Bone Marrow: BM
*Cd79a* gene encoding the immunoglobulin-alpha subunit of the B lymphocyte antigen receptor: CD79
Follicular B cells: FOB
Hypoxia-inducible Factor : HIF
Marginal Zone B cells : MZB
Myocardial infarction: MI
Recombination Signal Binding Protein For Immunoglobulin Kappa J Region : RbpjK
Toll-like receptor: TLR
Wild-type: WT

**Introduction**

Numerous biological mechanisms converge to remodel the heart after myocardial infarction (MI). Adverse post-ischemic cardiac remodeling and progression to heart failure may be promoted by macroscopic alterations in left ventricle geometry and function, as well as microscopic alterations in the cellular and molecular landscapes of the ischemic heart. Recent evidence implicates both infiltrated and resident immune cells in post-MI remodeling (1) (2). Notably, B lymphocytes have been shown to produce the chemokine CCL7 and promote cardiac inflammatory monocyte recruitment after acute MI, leading to enhanced tissue damage and myocardial dysfunction (3). Likewise, rapid elimination of cardiac B cells along with reduced CCL7 expression prevented pathological remodeling and heart failure (4). Modulation of different subsets of B lymphocytes has also been shown to control tissue remodeling in different experimental models of cardiac disease (5) (6) (7). Large B cell clusters were identified in epicardial adipose tissue of patients with coronary artery disease and in infarcted mice. B cell depletion reduced cardiac neutrophil infiltration as well as fibrosis and preserved left ventricular ejection fraction after acute MI (8). Conversely, IL-10–producing $CD5^+$ B cells were expanded in pericardial adipose tissues and activated the resolution of MI-induced inflammation (9). Altogether, these results indicate that B cells control left ventricle remodeling but the cellular mechanisms governing the effects of distinct B lymphocyte subtypes from diverse tissue origin remain to be defined. This is highly important given the ongoing and planned clinical trials aiming at targeting B cells in patients with acute MI (10).

MicroRNAs (miR) are fundamental to the development of inflammatory cells and also capable of regulating almost every leukocyte-related activity. Notably, they play prominent roles in B cell maturation, and different stages of normal B cell differentiation are characterized by distinct miRNA expression profiles (11) (12). Among these miRs, several

reports have demonstrated a key role for miR21 in inflammatory cells and increased miR21 expression is coupled with conditions involving altered immune response including cardiovascular diseases (13). In B cells, overexpression of miR21 leads to a pre-B malignant lymphoid-like phenotype, suggesting that miR21 may act as an oncogene in B cells (14).
In the present study, we reveal, for the first time, the involvement of splenic marginal zone B cells in the regulation of cardiac function and remodeling after acute MI. We also show that endogenous activation of miR21/Hypoxia-inducible factor(HIF)1$\alpha$-related pathway is an integral component of splenic marginal zone B cell-dependent damaging effect on post-ischemic cardiac remodeling.

**Methods**

*Experimental procedure*

All experiments were conducted according to the ethical committee for animal experimentation (University of Paris, CEEA 34) and the National Charter on the ethics on animal experimentation from the French Minister of Higher Education and Research under the reference MESR: n° 01373.01. Acute MI was induced by permanent ligation of the left anterior descending coronary artery (LAD) in mice. Cardiac function and remodeling were analyzed using echocardiography and immunohistochemistry. For evaluation of the role of HIF-1$\alpha$ and HIF-2$\alpha$ in B cells: $Cd79a^{cre/+}$ mice were crossed with $Hif1a^{flox/flox}$ and/or $Hif2a^{flox/flox}$ animals to generate $Cd79a^{cre/+}/Hif1a^{flox/flox}$ (referred to as the $Hif1a^{-/-}$ B cell group); $Cd79a^{cre/+}/Hif2a^{flox/flox}$ (referred to as the $Hif2a^{-/-}$ B cell group); $Cd79a^{cre/+}/Hif1a\text{-}Hif2a^{flox/flox}$ (referred to as the $Hif1a\text{-}2a^{-/-}$ B cell group) mice and their littermates $Cd79a^{+/+}/Hif1a^{flox/flox}$, $Cd79a^{+/+}/Hif2a^{flox/flox}$ or $Cd79a^{+/+}/Hif1a\text{-}Hif2a^{flox/flox}$ (referred to as the WT B cell groups). For evaluation of the role of MZB cells, $Cd79a^{cre/+}$ animals were crossed with $Rbpjk^{flox/flox}$ mice to generate $Cd79a^{cre/+}/Rbpjk^{flox/flox}$ (referred to as the $MZB^{\Delta}$ group lacking MZB cells) and $Cd79a^{+/+}/Rbpjk^{flox/flox}$ (referred to as the $MZB^{WT}$ group) animals.

*Statistical analysis*

Kruskal-Wallis one-way analysis of variance was used to compare three or more independent experimental groups. Comparisons between groups were then performed using Dunn's multiple comparisons test when the analysis of variance test was statistically significant. Mann-Whitney Test was used to compare two groups. A p value $<0.05$ was considered significant. Results are expressed as means with standard deviations or as boxes and whiskers with maximum and minimum values. P values presented in this report have not been adjusted for multiplicity, and therefore inferences drawn from these statistics may not be reproducible. A detailed description of all experimental procedures is provided in the supplemental Appendix.

**Results**

***Role of B cell specific miR21 in the response to acute MI***

As mature B cells mainly reside in the spleen, we first assessed miR21 expression in the spleen of wild-type (WT) mice, which were sham-operated or subjected to a permanent LAD ligation to induce acute MI, at different time-points after the onset of ischemia. We found that miR21 was upregulated at day 1 after the ischemic insult in the spleen, when compared to sham-operated animals (Figure 1A). Using FACS analysis, we then determined miR21 levels in distinct splenic inflammatory cells at day 1 after MI and showed that miR21 was strongly expressed in B cells when compared to other types of splenic inflammatory cells, including neutrophils, T lymphocytes, monocytes and macrophages (Figure 1A). Splenic B cells are known to emerge from B cell progenitors within the bone marrow (BM) and subsequently to undergo final maturation in the spleen (15). To assess the role of miR21 in mediating B cell dependent effects on post-MI cardiac remodeling, we generated WT chimeras through lethal irradiation and reconstitution with BM cells isolated from WT or miR21-deficient animals. Transplantation of miR21 deficient BM did not impact the number of splenic B cells (Figure

1B) but reduced miR21 levels in splenic B cells when compared to mice transplanted with WT BM (Figure 1C). Left ventricular ejection fraction was similar in both un-operated and sham-operated chimeric animals (Supplemental Figure 1A). After induction of acute MI, cardiac function was higher in WT mice reconstituted with *miR21*$^{-/-}$ BM cells when compared to WT chimeras (Figure 1D). Interstitial fibrosis was 1.7-fold lower in WT mice reconstituted with *miR21*$^{-/-}$ BM compared to those receiving WT BM (Figure 1E). Infarct size and capillary density were unaffected (Figure 1E). We also substantiated the role of B cell specific miR21 in re-supplementation experiments using B cell transplantation in immunodeficient animals (Supplemental results and Supplemental Figure 1B-D). Altogether, these results indicate that miR21 controls B cell-dependent impact on post-ischemic cardiac remodeling.

***B cell specific miR21 impacts the inflammatory response post-MI***

Toll-like receptor (TLR) activation has been shown to trigger CCL7 secretion by B cells and governs bone marrow derived monocyte mobilization and infiltration in the ischemic milieu (3) (4). Increased miR21 expression is also associated with TLR activation (16). Treatment with TLR agonist, CpG, for 24 hours led to a 1.8-fold increase of miR21 expression in cultured splenic B cells (Figure 1F). CpG stimulation was also associated with activation of CCL7 production by cultured WT B cells, and this effect was blunted in cultured B cells isolated from *miR21*$^{-/-}$ mice (Figure 1G). CCL7 circulating levels were reduced in chimeric *miR21*$^{-/-}$ animals at day 3 after MI (Figure 1H). We then evaluated the impact of CCL7 alteration on the number of monocytes (3) (17). Within the population of $CD45^{+}CD11b^{+}Ly6G^{-}$ cells, classical inflammatory monocytes were characterized as $Ly6C^{High}$ cells (Supplemental Figure 2). miR21 deficiency was associated with a reduction in both circulating and cardiac $Ly6C^{High}$ monocytes (Figure 1I). Re-supplementation experiments using WT and miR21-deficient B cells also revealed variation of CCL7 and inflammatory

monocyte levels (Supplemental results and Supplemental Figure1E-F). Thus, miR21 expression fosters CCL7 production by activated B cells, which promotes mobilization and infiltration of Ly6C$^{High}$ monocytes leading to adverse ventricular remodeling and cardiac dysfunction.

***miR21 controls HIF-1α levels in B cells***

MiR21 has been shown to enhance hypoxia inducible factor-1 (HIF-1)α signaling (18) (19) (20). HIF-1α is a master transcription factor that controls B cell function (21) (22) (23). Interestingly, aberrant regulation of HIF-1α by miRNAs is a hallmark of chronic lymphocytic leukemia B cells (24). HIF-1α also drives B cell-related effects in exacerbated collagen-induced arthritis and experimental autoimmune encephalomyelitis (25). We then speculated that miR21-induced regulation of HIF-1α controlled B cell related effects on post-ischemic cardiac homeostasis. For this purpose, HIF-1α levels were examined in splenic B cell isolated from WT and *miR21*$^{-/-}$ mice and stimulated with CpG or anti-IgM. Upregulation of HIF-1α protein content was blunted in activated *miR21*$^{-/-}$ B cells when compared to activated WT B cells (Figure 2A).

***HIF-1α mediates B cell-related effects in mice with acute MI***

To evaluate, the role of HIF-1α in B cells, we generated mice with B cell lineage specific conditional deletion of HIF1α (*Hif1a*$^{-/-}$ B cells). HIF1α deficiency did not affect cardiac function in un-operated and sham-operated animals (Supplemental Figure 3A). After MI, mice with *Hif1a*$^{-/-}$ B cells showed improved cardiac function when compared to WT animals (Figure 2B). Cardiac function recovery was associated with reduction in both infarct size and interstitial fibrosis whereas capillary density was unaffected (Figure 2B). HIF-1α invalidation did not reduce total B cell number in the spleen after MI (Figure 3A). CCL7 levels were decreased in blood of mice with *Hif1a*$^{-/-}$ B cells (Figure 3B). CpG treatment increased HIF-1 α transcriptional activity (Figure 3C) as well as CCL7 mRNA and proteins levels (Figure 3D)

in WT cultured B cells. Of note, CCL7 upregulation was abrogated in cultured *Hif1a*$^{-/-}$ B cells treated with CpG (Figure 3D). As a consequence, the number of Ly6C$^{High}$ monocytes was lowered in the blood and the infarcted heart (Figure 3E). Similarly, cardiac macrophage accumulation (gating strategy is shown in Supplemental Figure 2) as well as the expression of classical pro-inflammatory cytokines such as IL1ß and IL6, were reduced in mice with *Hif1a*$^{-/-}$ B cells when compared to WT animals, at day 7 after MI (Figure 3F).

***HIF-2α is not involved in B cell-related effects post-MI***

In mammalian cells, HIFα activity is mainly regulated by two α subunits, HIF-1α and HIF-2α. Although HIF-1α and HIF-2α are paralogs and share extensive sequence homology, these two α subunits have also non-overlapping and sometimes even opposing roles (26). Furthermore, HIF-1α deficiency has also been shown to increase levels of HIF-2α and mutual antagonism between HIFα isoforms can shape HIFα activity (27). We found that *Hif2a* mRNA levels were enhanced in *miR21*$^{-/-}$ and *Hif1a*$^{-/-}$ splenic B cells, 1 day after the onset of ischemia (Supplemental Figure 3B). Cardiac function and post-MI remodeling were similar in mice with *Hif2a*$^{-/-}$ B cells and their WT littermates as well as in un-operated and sham-operated animals (Supplemental Figure 3C-D). On the same note, *Hif2a* deletion did not impact B cell numbers in the spleen, did not modulate blood CCL7 levels and did not alter circulating and cardiac Ly6C$^{High}$ monocyte number (Supplemental Figure 3 E-G). In contrast, whereas cardiac function was similar in un-operated and sham-operated animals (Supplemental Figure 3H), *Hif1a* and *Hif2a* deletion improved cardiac function after MI (Figure 4A). Cardiac function recovery was associated with reduction in infarct size whereas interstitial fibrosis and capillary densities were unaffected (Figure 4A). *Hif1a and Hif2a* deficiency also reduced Ly6C $^{High}$ monocytes and CCL7 levels in the blood along with a reduction of cardiac macrophage number and *Il1ß* and *Il6* mRNA levels (Figure 4B-E). Altogether, these results indicate that HIF-2α does not control B cell related functions and that HIF-1α isoform plays a

prominent role in the orchestration of B cell-induced deleterious effects on post-MI cardiac remodeling.

***Marginal zone B cells are instrumental in the regulation of cardiac function and remodeling post-MI***

Several subsets of B cells exist. They are broadly divided into innate-like B1 cells and B2 cells, which comprise marginal zone (MZB) and follicular B cells (FOB) with specific developmental pathways and functional properties (15). Within the population of $IgM^{+}CD19^{+}$ B cells, MZB cells were identified as $CD23^{low/-}CD21^{high}$, and FOB cells as $CD23^{high}CD21^{low/-}$ (Supplemental Figure 2). MZB cells displayed higher expression of miR21 when compared to FOB cells and miR21 expression was markedly upregulated in MZB cells of infarcted animals when compared to sham-operated mice (Figure 5A). To determine the specific role of MZB cells, we then used mice with MZB cell deficiency ($MZB^{\Delta}$) (28). As expected, MZB cell number was markedly decreased in the spleen of $MZB^{\Delta}$ mice (Figure 5B). Interestingly, MZB cell deficiency curbed MI-induced miR21 upregulation in splenic B cells (Figure 5C). Cardiac function was similar in un-operated and sham-operated $MZB^{\Delta}$ and $MZB^{WT}$ animals (Supplemental Figure 3I). The selective depletion of MZB cells improved post-MI cardiac function and the remodeling process (Figure 5D-G), suggesting that MZB cells expressing miR21 played a significant role in the regulation of cardiac function and repair. On the same note, CpG stimulation enhanced CCL7 release in cultured $MZB^{WT}$ cells but not in $MZB^{\Delta}$ cells (Figure 6A). MZB cell-deficient mice also displayed altered circulating levels of CCL7 (Figure 6B) and reduced circulating and cardiac $Ly6C^{High}$ monocytes when compared to their wild-type littermates (Figure 6C). As a consequence, at day 7 after MI, the number of cardiac macrophages as well as *Il1b* and *Il6* mRNA levels were decreased in the infarcted hearts of $MZB^{\Delta}$ mice when compared to $MZB^{WT}$ animals (Figure 6D). In additional set of experiments, we challenged WT and MZB cell-deficient animals with a sequence of ischemia-reperfusion

for 40 minutes. MZB cell deficiency also improved cardiac function and reduced interstitial fibrosis in this experimental setting (Supplemental Figure 4).

***miR21/HIF1α signaling controls marginal zone B cell-related effects in mice with acute MI***

We then assessed the role of miR21/HIF1α signaling selectively in MZB cells. CpG- and IgM- induced HIF-1α upregulation was abrogated in B cells isolated from $MZB^{\Delta}$ mice when compared to those isolated from $MZB^{WT}$ animals (Figure 7A). To substantiate the role of miR21 in HIF-1α regulation within MZB cells, we cultured FOB and MZB cells from WT and *miR21* deficient mice and analyzed HIF1α protein levels (Figure 7B). We showed that miR21 deficiency hampered CpG and IgM-induced upregulation of HIF-1α protein levels and CCL7 release in MZB but not in FOB cultured cells (Figure 7B). Finally, we generated chimeric mice in which MZB deficient mice have been partially irradiated and reconstituted with BM cells isolated from $MZB^{\Delta}$, $MZB^{WT}$, $miR21^{-/-}$ or $Hif1a^{-/-}$ animals. Reconstitution restored the number of MZB cells in chimeric animals (Figure 7C) without affecting cardiac function in un-operated and sham-operated animals (Supplemental Figure 5A). Chimeric mice transplanted with MZB $miR21^{-/-}$ cells displayed reduction of miR21 content in MZB cells (Supplemental Figure 5B) whereas chimeric mice transplanted with MZB $Hif1a^{-/-}$ cells showed decreased *Hif1a* mRNA levels in MZB cells (Supplemental Figure 5B-C). miR21 and *Hif1a* mRNA levels were unaffected in FOB cells in chimeric mice (Supplemental Figure 5B-C). Of great interest, transplantation with WT, miR21-deficient MZB or *Hif1a*-deficient MZB cells reduced circulating CCL7 levels and improved cardiac function when compared to chimeric $MZB^{\Delta}$ animals (Figure 7C-D). These effects were associated with reduction in infarct size and (Figure 7D), interstitial fibrosis, cardiac macrophage as well as *Il1ß* and *Il6* mRNA contents (Supplemental Figure 5 D-F).

Thus, miR21 expression controls HIF-1$\alpha$ content in activated MZB cells and MZB cells govern inflammation-dependent ventricular remodeling and cardiac function (Central illustration).

**Discussion**

In the present work, we demonstrated that deletion of MZB cells or selective miR21 deficiency in MZB cells abrogated B cell-induced adverse ventricular remodeling after MI, indicating a determinant role for miR21-expressing MZB cells in this context. Although previously unsuspected, this new role of MZB cells in the response to acute ischemic injury is consistent with their innate-like properties and their strategic positioning at the blood-lymphoid interface, where they can sense changes in the systemic environment and mount immediate innate immune responses. miR21 up-regulation was correlated with activation of HIF-1α related signaling and conditional deletion of HIF-1α counteracted MZB cell-induced adverse cardiac remodeling and dysfunction. In mature B cells, persistent (re)-induction of HIF transcription factors limits proliferation, isotype switching, and levels of high-affinity antibodies in splenic germinal centers after immunization (29). It is unlikely that those adaptive B cell functions were involved in our experimental conditions very shortly after ischemic injury. However, one can speculate that dying cells and matrix fragments within the ischemic infarcted milieu may produce specific signals, including cytokines or damage-associated molecular patterns, and activate innate-like MZB cells. In this line of reasoning, TLR activation is sufficient to activate the miR21/HIF-1α pathway in cultured MZB cells. Nevertheless, further investigations are needed to elucidate how B cells are able to recognize these specific biological entities originating from the injured myocardium and how the ischemic milieu commands B cell effector functions. Our work also identifies a determinant role for miR21 and HIF-1α in the regulation of CCL7 production by MZB cells. CCL7 directs $Ly6C^{High}$ monocyte mobilization from the bone marrow and recruitment to inflammatory

cardiac tissue (3) (30). Ly6C$^{High}$ pro-inflammatory monocytes are responsible for the scavenging of debris and secretion of pro-inflammatory cytokines and matrix-degrading proteases, which contribute to the myocardial injury (3) (17). Of note, bioinformatic analysis and chromatin immunoprecipitation assays revealed three functional hypoxia-response elements in the *Ccl7* promoter, indicating that *Ccl7* is a direct HIF-1α target gene (31). However, additional work will be required to deeply address the mechanisms through which miR21 and HIF-1α regulate CCL7 production.

As B cells have emerged as important players in atherogenesis and post-MI cardiac remodeling, our novel results add to a number of experimental and clinical evidence suggesting that B cells represent a promising therapeutic target for cardiovascular diseases. Several B cell-directed therapies are already available such as rituximab, an anti-CD20 B cell depleting monoclonal antibody. Small-scale human studies have previously reported some beneficial effects on the cardiovascular system such as variable degrees of reduction in carotid intima-media thickness, improved flow-mediated dilation or decreased arterial thickness in rituximab-treated patients (32). Recently, we have conducted a phase 1/2 clinical trial investigating the impact of rituximab in patients with acute MI, and showed that infusion of rituximab within 24 hours of MI was safe and efficiently depleted circulating B cells (10). The detrimental role of MZB cells at the acute phase of MI shown in the present study contrasts with their previously reported atheroprotective properties through modulation of T follicular helper cell functions (28). What are therefore the clinical implications of these opposing properties? We propose that a therapeutic strategy that depletes MZB cells needs to be both selective and limited to the acute phase after MI, allowing for MZB cell recovery after the acute phase and reducing any potential harm, which can result from a loss of their atheroprotective properties. The B cell depleting strategy currently being tested at the acute phase of MI in humans uses one single infusion of rituximab (10). Rituximab depletes both

FOB and MZB cells. It is interesting to note, however, that transitional B cells with innate-like immune properties appear to recover after a few months of a single low-dose rituximab (10), suggesting that a low dose may limit the loss of potentially atheroprotective B cells. Besides, selective targeting of miR21 or HIF-1α signaling in MZB cells, which would probably not impact the atheroprotective properties of MZB cells, would be another potential therapeutic strategy in patients with acute MI

Study limitations

This study did not attempt to identify the specific cardiac derived signals that could activate miR21/HIF-1α signaling in MZB cells. It is also likely that miR21 and HIF-1α control additional targets that could modulate splenic, circulating or cardiac B cell related effects.

Conclusion

This work reveals a prominent role for the miR21/HIF-1α axis in guiding MZB cell function in response to MI through activation of CCL7-dependent mobilization and infiltration of pro-inflammatory monocytes into the ischemic myocardium.

**Perspectives**

COMPETENCY IN MEDICAL KNOWLEDGE: Acute MI induces activation of miR21/HIF1-α signaling in splenic marginal zone B cells, leading to the release of the chemoattractant cytokine CCL7 that fosters inflammatory monocyte infiltration in the cardiac tissue and precipitates adverse left ventricular remodeling and cardiac dysfunction.

TRANSLATIONAL OUTLOOK: Targeting B lymphocytes could represent a therapeutic opportunity to limit adverse ventricular remodeling after MI. This strategy is currently under investigation in patients with acute MI.

**References**


1. Frangogiannis NG. The inflammatory response in myocardial injury, repair, and remodelling. Nat Rev Cardiol. 2014;11:255-65.
2. Yu X, Newland SA, Zhao TX et al. Innate Lymphoid Cells Promote Recovery of Ventricular Function After Myocardial Infarction. J Am Coll Cardiol. 2021;78:1127-1142.
3. Zouggari Y, Ait-Oufella H, Bonnin P et al. B lymphocytes trigger monocyte mobilization and impair heart function after acute myocardial infarction. Nat Med. 2013;19:1273-80.
4. Luk FS, Kim RY, Li K et al. Immunosuppression With FTY720 Reverses Cardiac Dysfunction in Hypomorphic ApoE Mice Deficient in SR-BI Expression That Survive Myocardial Infarction Caused by Coronary Atherosclerosis. J Cardiovasc Pharmacol. 2016;67:47-56.
5. Adamo L, Staloch LJ, Rocha-Resende C et al. Modulation of subsets of cardiac B lymphocytes improves cardiac function after acute injury. JCI Insight. 2018;3.
6. Adamo L, Rocha-Resende C, Lin CY et al. Myocardial B cells are a subset of circulating lymphocytes with delayed transit through the heart. JCI Insight. 2020;5.
7. Cordero-Reyes AM, Youker KA, Trevino AR et al. Full Expression of Cardiomyopathy Is Partly Dependent on B-Cells: A Pathway That Involves Cytokine Activation, Immunoglobulin Deposition, and Activation of Apoptosis. J Am Heart Assoc. 2016;5.
8. Horckmans M, Bianchini M, Santovito D et al. Pericardial Adipose Tissue Regulates Granulopoiesis, Fibrosis, and Cardiac Function After Myocardial Infarction. Circulation. 2018;137:948-960.
9. Wu L, Dalal R, Cao CD et al. IL-10-producing B cells are enriched in murine pericardial adipose tissues and ameliorate the outcome of acute myocardial infarction. Proc Natl Acad Sci U S A. 2019;116:21673-21684.
10. Zhao TX, Ur-Rahman MA, Sage AP et al. Rituximab in Patients with Acute ST-elevation Myocardial Infarction (RITA-MI): an Experimental Medicine Safety Study. Cardiovasc Res. 2021.
11. Koralov SB, Muljo SA, Galler GR et al. Dicer ablation affects antibody diversity and cell survival in the B lymphocyte lineage. Cell. 2008;132:860-74.
12. Zhang J, Jima DD, Jacobs C et al. Patterns of microRNA expression characterize stages of human B-cell differentiation. Blood. 2009;113:4586-94.
13. Dai B, Wang F, Nie X et al. The Cell Type-Specific Functions of miR-21 in Cardiovascular Diseases. Front Genet. 2020;11:563166.
14. Medina PP, Nolde M, Slack FJ. OncomiR addiction in an in vivo model of microRNA-21-induced pre-B-cell lymphoma. Nature. 2010;467:86-90.
15. Pillai S, Cariappa A. The follicular versus marginal zone B lymphocyte cell fate decision. Nat Rev Immunol. 2009;9:767-77.
16. Sheedy FJ, Palsson-McDermott E, Hennessy EJ et al. Negative regulation of TLR4 via targeting of the proinflammatory tumor suppressor PDCD4 by the microRNA miR-21. Nat Immunol. 2010;11:141-7.
17. Nahrendorf M, Swirski FK. Monocyte and macrophage heterogeneity in the heart. Circ Res. 2013;112:1624-33.
18. Meng F, Henson R, Wehbe-Janek H, Ghoshal K, Jacob ST, Patel T. MicroRNA-21 regulates expression of the PTEN tumor suppressor gene in human hepatocellular cancer. Gastroenterology. 2007;133:647-58.

19. Liu LZ, Li C, Chen Q et al. MiR-21 induced angiogenesis through AKT and ERK activation and HIF-1alpha expression. PLoS One. 2011;6:e19139.
20. Richart A, Loyer X, Neri T et al. MicroRNA-21 coordinates human multipotent cardiovascular progenitors therapeutic potential. Stem Cells. 2014;32:2908-22.
21. Kojima H, Kobayashi A, Sakurai D et al. Differentiation stage-specific requirement in hypoxia-inducible factor-1alpha-regulated glycolytic pathway during murine B cell development in bone marrow. J Immunol. 2010;184:154-63.
22. Shin DH, Lin H, Zheng H et al. HIF-1alpha-mediated upregulation of TASK-2 K(+) channels augments Ca(2)(+) signaling in mouse B cells under hypoxia. J Immunol. 2014;193:4924-33.
23. Lall R, Ganapathy S, Yang M et al. Low-dose radiation exposure induces a HIF-1-mediated adaptive and protective metabolic response. Cell Death Differ. 2014;21:836-44.
24. Ghosh AK, Shanafelt TD, Cimmino A et al. Aberrant regulation of pVHL levels by microRNA promotes the HIF/VEGF axis in CLL B cells. Blood. 2009;113:5568-74.
25. Meng X, Grotsch B, Luo Y et al. Hypoxia-inducible factor-1alpha is a critical transcription factor for IL-10-producing B cells in autoimmune disease. Nat Commun. 2018;9:251.
26. Imtiyaz HZ, Williams EP, Hickey MM et al. Hypoxia-inducible factor 2alpha regulates macrophage function in mouse models of acute and tumor inflammation. J Clin Invest. 2010;120:2699-714.
27. Yuan G, Peng YJ, Reddy VD et al. Mutual antagonism between hypoxia-inducible factors 1alpha and 2alpha regulates oxygen sensing and cardio-respiratory homeostasis. Proc Natl Acad Sci U S A. 2013;110:E1788-96.
28. Nus M, Sage AP, Lu Y et al. Marginal zone B cells control the response of follicular helper T cells to a high-cholesterol diet. Nat Med. 2017;23:601-610.
29. Cho SH, Raybuck AL, Stengel K et al. Germinal centre hypoxia and regulation of antibody qualities by a hypoxia response system. Nature. 2016;537:234-238.
30. Tsou CL, Peters W, Si Y et al. Critical roles for CCR2 and MCP-3 in monocyte mobilization from bone marrow and recruitment to inflammatory sites. J Clin Invest. 2007;117:902-9.
31. Qi D, Wei M, Jiao S et al. Hypoxia inducible factor 1alpha in vascular smooth muscle cells promotes angiotensin II-induced vascular remodeling via activation of CCL7-mediated macrophage recruitment. Cell Death Dis. 2019;10:544.
32. Porsch F, Binder CJ. Impact of B-Cell-Targeted Therapies on Cardiovascular Disease. Arterioscler Thromb Vasc Biol. 2019;39:1705-1714.

**Figure Legends**

**Figure 1: Acute myocardial infarction upregulates miR21 levels in splenic B lymphocytes.**

**(A)** miR21 was increased in the spleen (n=6) and in splenic immune cells (n=4), at day 1 after MI (**P<0.01). Whereas splenic B cell number was similar **(B)**, miR21 levels **(C)** were reduced in chimeric animals (n=5, ***p<0.001). Ejection fraction **(D)** was increased whereas interstitial fibrosis **(E)** was reduced in WT:*miR21*$^{-/-}$ mice, at day 14 after MI (n=8, from 2 independent experiments, *P<0.05, **P<0.01). CpG enhanced miR21 levels **(F)** and CCL7 release **(G)** in cultured WT B cells (n=5, *P<0.05 versus non-stimulated WT B cells, †P<0.05 versus CpG treated WT B cells). CCL7 **(H)** and Ly6C$^{High}$ monocyte levels **(I)** in blood (left) and cardiac tissue (right) were reduced in WT:*miR21*$^{-/-}$ animals (n=6, *P<0.05,**P<0.01). *Abbreviations:* NS indicates non-stimulated; nd not detected; Sham, sham-operated animals; WT:WT or WT:*miR21*$^{-/-}$ chimeric mice transplanted with BM derived cells isolated from WT or miR21$^{-/-}$ animals, respectively. No corrections for multiple testing were applied.

**Figure 2: Improved cardiac function in mice with *Hif1a* deletion in B cells.**

**(A)** Representative photomicrographs (left) and quantitative evaluation (right) of western-blot experiments showed increased HIF-1α protein levels in spleen-derived B cells (*P<0.05 versus CpG treated WT B cells, †P<0.05 versus anti-IgM treated WT B cells). **(B)** *Hif1a* deficiency in B cells improved ejection fraction and reduced infarct size as well as interstitial fibrosis. Representative images used for quantification are also shown (n=15, from 2 independent experiments, *P<0.05, **P<0.01 versus WT B cells). *Abbreviations:* Anti-IgM indicates goat anti-mouse IgM antibody; CpG, TLR agonist; CTL, control non stimulated B cells; DMOG, inhibitor of HIF1α degradation Dimethyloxaloylglycine; *Hif1a*$^{-/-}$ B cells, mice with conditional deletion of *Hif1a* in B cells and WT B cells, their wild-type littermates. No corrections for multiple testing were applied.

**Figure 3: HIF1α expression in B cells controls inflammatory reaction.**

**(A)** *Hif1a* deletion in B cells did not impact the number of splenic B cells (n=5) but **(B)** reduced CCL7 protein levels (n=4, **P<0.01). CpG treatment increased HIF-1α transcriptional activity **(C)** as well as CCL7 mRNA and proteins levels **(D)** in WT cultured B cells (n=5, *P<0.05,**P<0.01 versus non-stimulated B cells; †P<0.05 versus CpG treated WT B cells). *Hif1a* deletion in B cells decreased Ly6C$^{High}$ monocyte population **(E)** in blood (Left) and heart (Right), cardiac macrophage number as well as *Il1ß* and *Il6* mRNA levels **(F)** (n=6-8, *P<0.05, **P<0.01). *Abbreviations:* CpG indicates TLR agonist CpG; NS, non-stimulated B cells; DMOG, inhibitor of HIF1α degradation Dimethyloxaloylglycine; *Hif1a*$^{-/-}$ B cells, mice with conditional deletion of *Hif1a* in B cells and WT B cells, their wild-type littermates. . No corrections for multiple testing were applied.

**Figure 4: HIF2α expression in B cells is dispensable for B cell-related effects.**

**(A)** Ejection fraction was increased and infarct size was diminished in *Hif1a-2a*$^{-/-}$ B cell group, at day 14 after MI. (n=16, from 2 independent experiments, **P<0.01). On the same note, CCL7 circulating levels **(B)**, blood Ly6C$^{High}$ monocyte number **(C)**, cardiac macrophage amount **(D)** as well as *Il1ß* and *Il6* mRNA levels **(E)** were reduced in *Hif1a-2a*$^{-/-}$ B cell group. (n=7, **P<0.01). *Abbreviations: Hif1a-2a*$^{-/-}$ B cells indicates mice with conditional deletion of *Hif1a* and *Hif2a* in B cells; WT B cells, their wild-type littermates. For panel D and E analysis have been performed at day 7 after MI. No corrections for multiple testing were applied.

**Figure 5: MZB cells are instrumental components of post-MI cardiac repair.**

**(A)** miR21 was mainly expressed in spleen derived MZB cells (n=4, *P<0.05 versus FOB WT mice) and was upregulated, 24 hours after MI (n=6, **P<0.01 versus MZB cells in sham mice). MZB deficient animals displayed reduced number of MZB cells **(B)** (n=4, **P<0.01 for MZB$^{\Delta}$ versus MZB$^{WT}$ mice) and miR21 levels **(C)** (n=6, *P<0.05, ***P<0.001 versus

sham mice, ††P<0.01 versus infarcted $MZB^{WT}$ mice). MZB cell deficiency improved ejection fraction (n=10 from 2 independent experiments) **(D)** and reduced infarct size, interstitial fibrosis **(E)**, *Col1a1* and *Col3a1* mRNA levels **(F)** without affecting capillary density **(G)** at day 14 after MI. (n=6, *P<0.05, **P<0.01). Representative images used for quantification are also shown. *Abbreviations:* FOB indicates follicular B cells; MZB, marginal zone B cells, $MZB^{\Delta}$ mice with conditional deletion of MZB cells and MZB $^{WT}$, their wild-type littermates; Sham, sham-operated animals. No corrections for multiple testing were applied.

**Figure 6: MZB cells control inflammatory reaction.**

**(A)** CCL7 release was increased in the supernatant of CpG-treated cultured B cells isolated from $MZB^{WT}$ animals (n=5, *P<0.05 versus non stimulated $MZB^{WT}$ cells, †P<0.05 versus CpG treated MZB $^{WT}$ cells). **B)** Accordingly, CCL7 protein levels were reduced in blood of $MZB^{\Delta}$ mice after MI (n = 6, **P<0.01). MZB deficiency hampered $Ly6C^{High}$ monocyte number in blood and cardiac tissue **(C)**, cardiac macrophage content as well as *Il1ß* and *Il6* mRNA levels **(D)** (*P<0.05, **P<0.01). *Abbreviations:* CpG indicates TLR agonist CpG; NS, non-stimulated B cells; MZB, marginal zone B cells, $MZB^{\Delta}$ mice with conditional deletion of MZB cells and $MZB^{WT}$, their wild-type littermates; Sham, sham-operated animals. For panel D analysis have been performed at day 7 after MI. No corrections for multiple testing were applied.

**Figure 7: miR21-HIF1α signaling shapes the deleterious effect of MZB cells.**

**(A)** CpG and IgM treatment improved HIF-1α protein levels in splenic WT B cells (**P<0.01 versus untreated B cells, †P<0.05 versus CpG treated $MZB^{\Delta}$ cells). **(B)** miR21 deficiency hampered CpG- and IgM-induced HIF-1α protein level upregulation and CCL7 release in splenic MZB cells (**P<0.01 versus WT FOB cells, ††P<0.01 versus WT MZB cells). **(C)** MZB cell number was reduced in chimeric $MZB^{\Delta}$ mice (n=7, ***P<0.001). Specific deletion of miR21 and *Hif1a* in MZB cells reduced blood CCL7 levels **(C)** improved ejection fraction

as well as reduced infarct size **(D)** (n=7, **P<0.01, ***P<0.001). *Abbreviations:* CTL, unstimulated B cells; FOB, follicular B cells; MZB, marginal zone B cells. $MZB^{\Delta}$:$MZB^{\Delta}$, chimeric marginal zone B cell deficient mice ($MZB^{\Delta}$); $MZB^{WT}$:$MZB^{\Delta}$, chimeric $MZB^{WT}$ mice; $MZB^{miR21-/-}$:$MZB^{\Delta}$ and $MZB^{Hif1a-/-}$:$MZB^{\Delta}$ chimeric mice harboring *miR21* and *Hif1a* deficiency in MZB cells, respectively. No corrections for multiple testing were applied.

**Central illustration: role of marginal zone B cells after acute myocardial infarction.** Splenic marginal zone B cells are instrumental in the regulation of cardiac function and remodeling after acute myocardial infarction. miR21/HIF-1$\alpha$ signaling adjusts the ability of marginal zone B cells to modulate CCL7 secretion and subsequently impact inflammatory monocyte-dependent cardiac remodeling after injury.

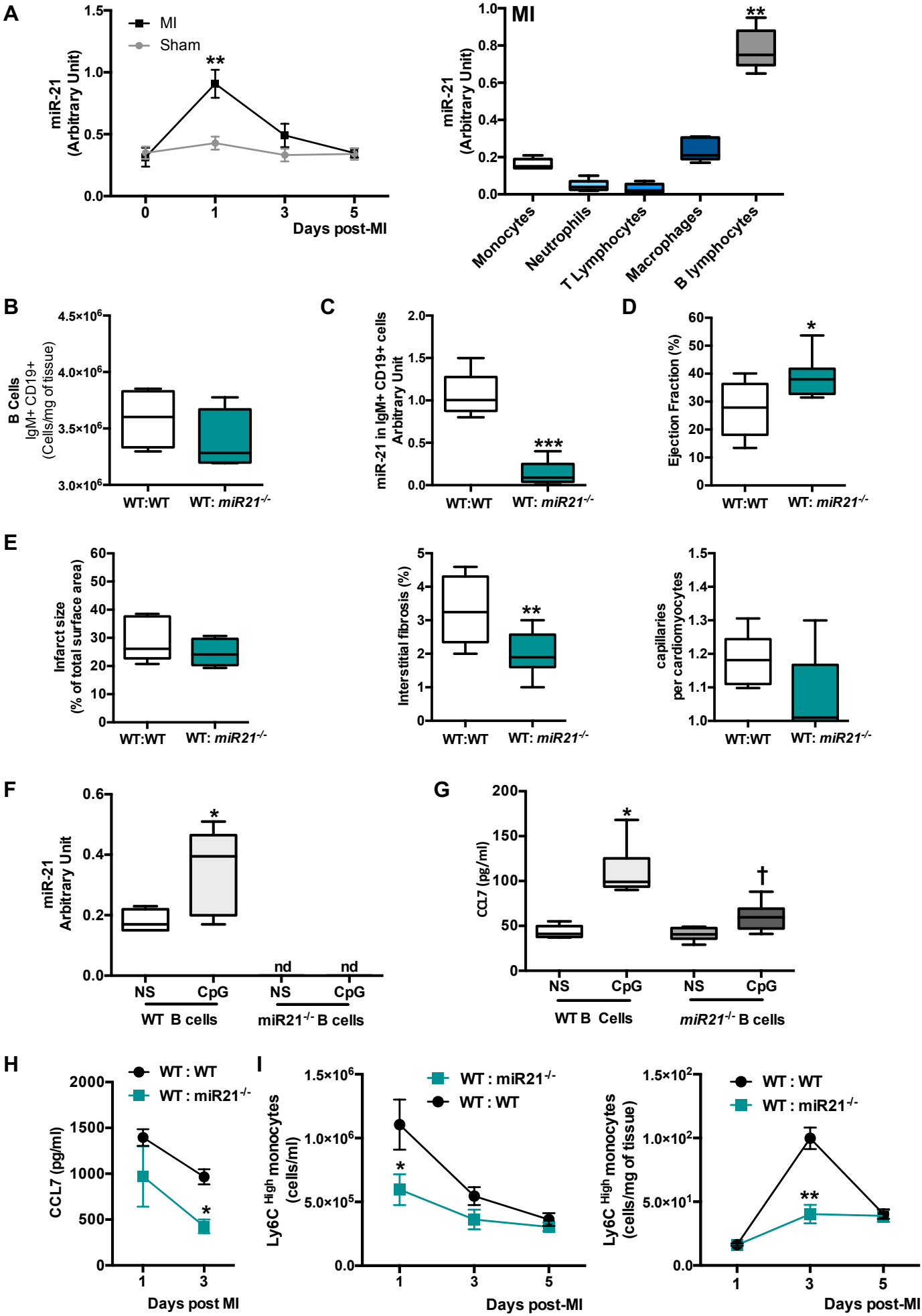
A
MI
Sham
miR-21 (Arbitrary Unit)
Days post-MI
MI
Monocytes
Neutrophils
T Lymphocytes
Macrophages
B lymphocytes
B
B Cells IgM+ CD19+ (Cells/mg of tissue)
WT:WT
WT: miR21-/-
C
miR-21 in IgM+ CD19+ cells Arbitrary Unit
D
Ejection Fraction (%)
E
Infarct size (% of total surface area)
Interstitial fibrosis (%)
capillaries per cardiomyocytes
F
miR-21 Arbitrary Unit
nd
NS
CpG
WT B cells
miR21-/- B cells
G
CCL7 (pg/ml)
WT B Cells
miR21-/- B cells
H
WT : WT
WT : miR21-/-
CCL7 (pg/ml)
Days post MI
I
Ly6C High monocytes (cells/ml)
Ly6C High monocytes (cells/mg of tissue)
Days post-MI

Figure 1

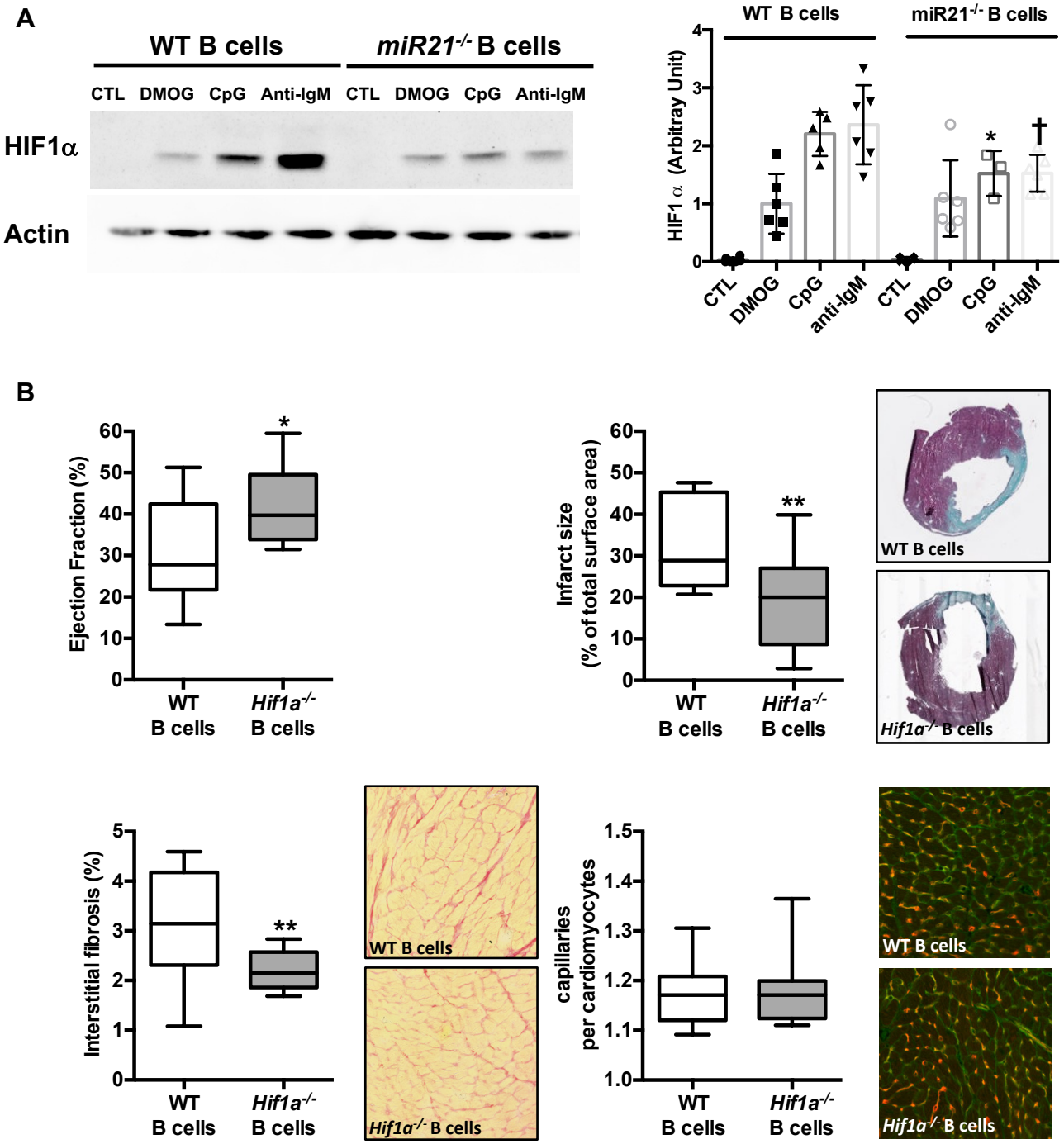
A
WT B cells
miR21-/- B cells
CTL DMOG CpG Anti-IgM CTL DMOG CpG Anti-IgM
HIF1α
Actin
WT B cells
miR21-/- B cells
HIF1 α (Arbitray Unit)
CTL DMOG CpG anti-IgM CTL DMOG CpG anti-IgM
B
Ejection Fraction (%)
WT B cells
Hif1a-/- B cells
Infarct size (% of total surface area)
WT B cells
Hif1a-/- B cells
WT B cells
Hif1a-/- B cells
Interstitial fibrosis (%)
WT B cells
Hif1a-/- B cells
WT B cells
Hif1α-/- B cells
capillaries per cardiomyocytes
WT B cells
Hif1a-/- B cells
WT B cells
Hif1α-/- B cells

Figure 2

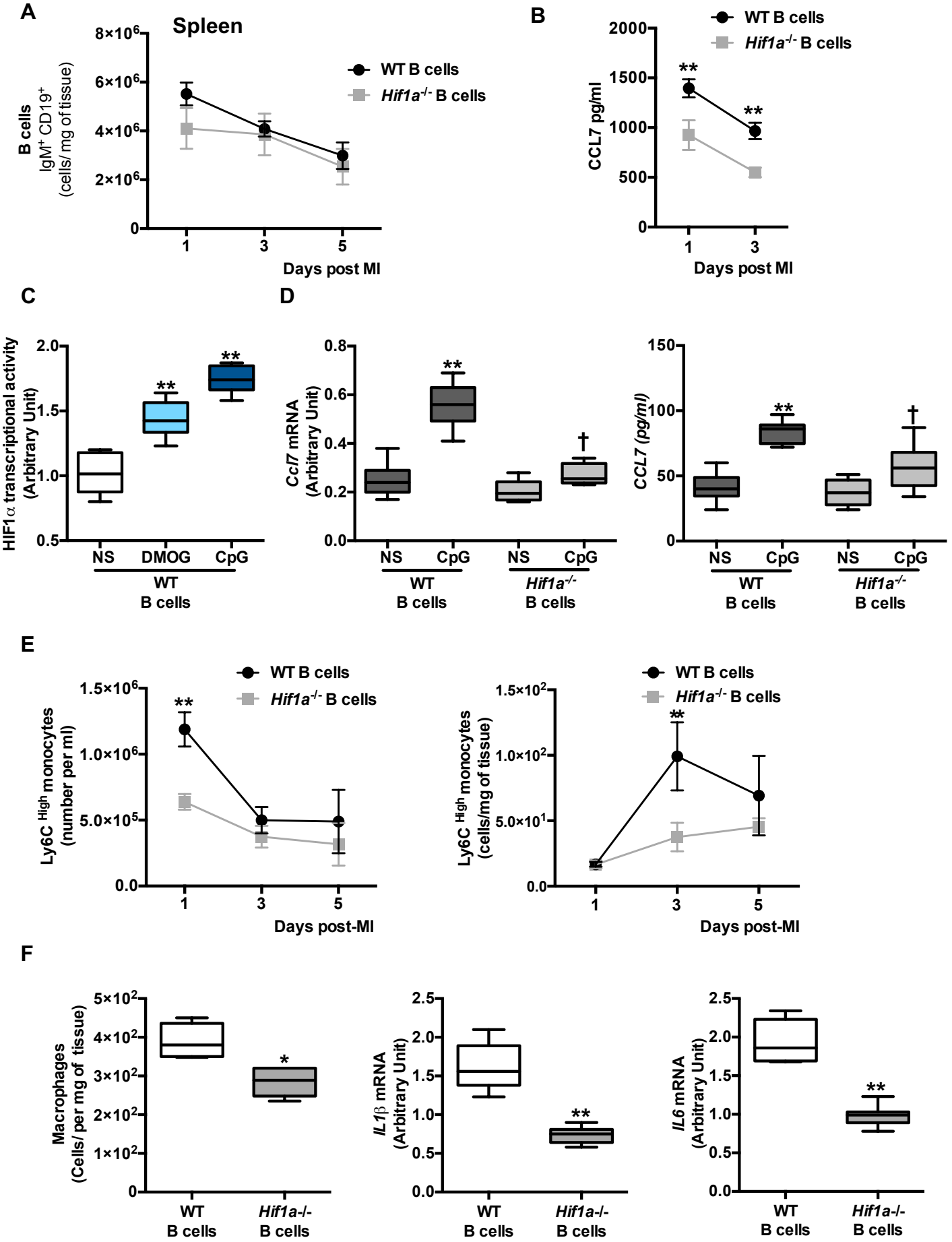
A
Spleen
B cells
IgM+ CD19+
(cells/ mg of tissue)
8×10^6
6×10^6
4×10^6
2×10^6
0
1
3
5
Days post MI
WT B cells
Hif1a-/- B cells
B
CCL7 pg/ml
2000
1500
1000
500
0
**
**
1
3
Days post MI
WT B cells
Hif1a-/- B cells
C
HIF1α transcriptional activity
(Arbitrary Unit)
2.0
1.5
1.0
0.5
**
**
NS
DMOG
CpG
WT
B cells
D
Ccl7 mRNA
(Arbitrary Unit)
0.8
0.6
0.4
0.2
0.0
**
†
NS
CpG
NS
CpG
WT
B cells
Hif1a-/-
B cells
CCL7 (pg/ml)
150
100
50
0
**
†
NS
CpG
NS
CpG
WT
B cells
Hif1a-/-
B cells
E
Ly6C High monocytes
(number per ml)
1.5×10^6
1.0×10^6
5.0×10^5
0.0
**
1
3
5
Days post-MI
WT B cells
Hif1a-/- B cells
Ly6C High monocytes
(cells/mg of tissue)
1.5×10^2
1.0×10^2
5.0×10^1
0.0
**
1
3
5
Days post-MI
WT B cells
Hif1a-/- B cells
F
Macrophages
(Cells/ per mg of tissue)
5×10^2
4×10^2
3×10^2
2×10^2
1×10^2
0
*
WT
B cells
Hif1a-/-
B cells
IL1β mRNA
(Arbitrary Unit)
2.5
2.0
1.5
1.0
0.5
0.0
**
WT
B cells
Hif1a-/-
B cells
IL6 mRNA
(Arbitrary Unit)
2.5
2.0
1.5
1.0
0.5
0.0
**
WT
B cells
Hif1a-/-
B cells

Figure 3

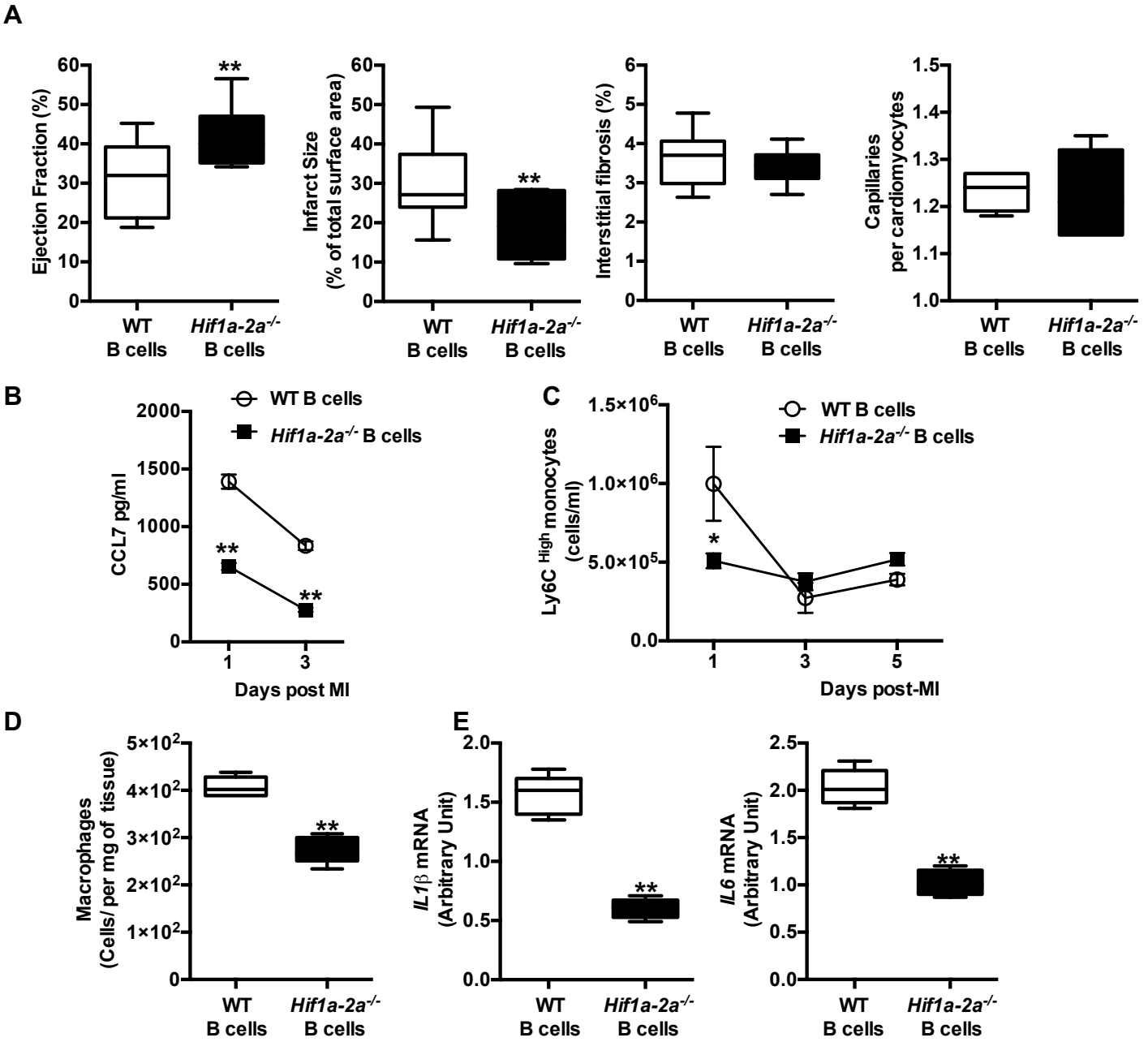
A
Ejection Fraction (%)
Infarct Size (% of total surface area)
Interstitial fibrosis (%)
Capillaries per cardiomyocytes
WT B cells
Hif1a-2a-/- B cells
B
WT B cells
Hif1a-2a-/- B cells
CCL7 pg/ml
Days post MI
C
Ly6C High monocytes (cells/ml)
Days post-MI
D
Macrophages (Cells/ per mg of tissue)
E
IL1β mRNA (Arbitrary Unit)
IL6 mRNA (Arbitrary Unit)

Figure 4

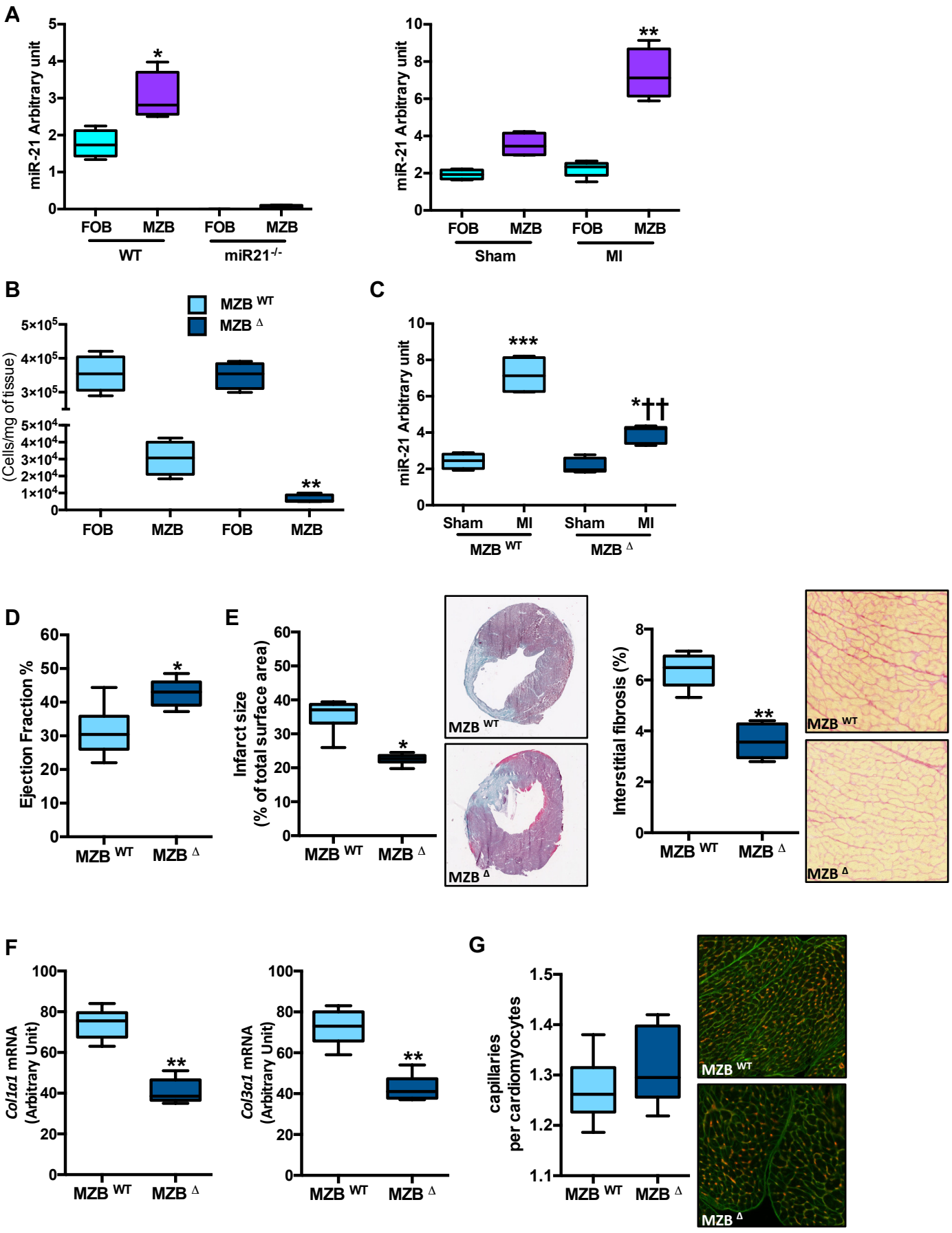
A
miR-21 Arbitrary unit
FOB
MZB
FOB
MZB
WT
miR21-/-
Sham
MI
B
MZB WT
MZB Δ
B Cells
(Cells/mg of tissue)
C
Sham
MI
MZB WT
MZB Δ
D
Ejection Fraction %
E
Infarct size
(% of total surface area)
Interstitial fibrosis (%)
F
Col1a1 mRNA
(Arbitrary Unit)
Col3a1 mRNA
(Arbitrary Unit)
G
capillaries
per cardiomyocytes

Figure 5

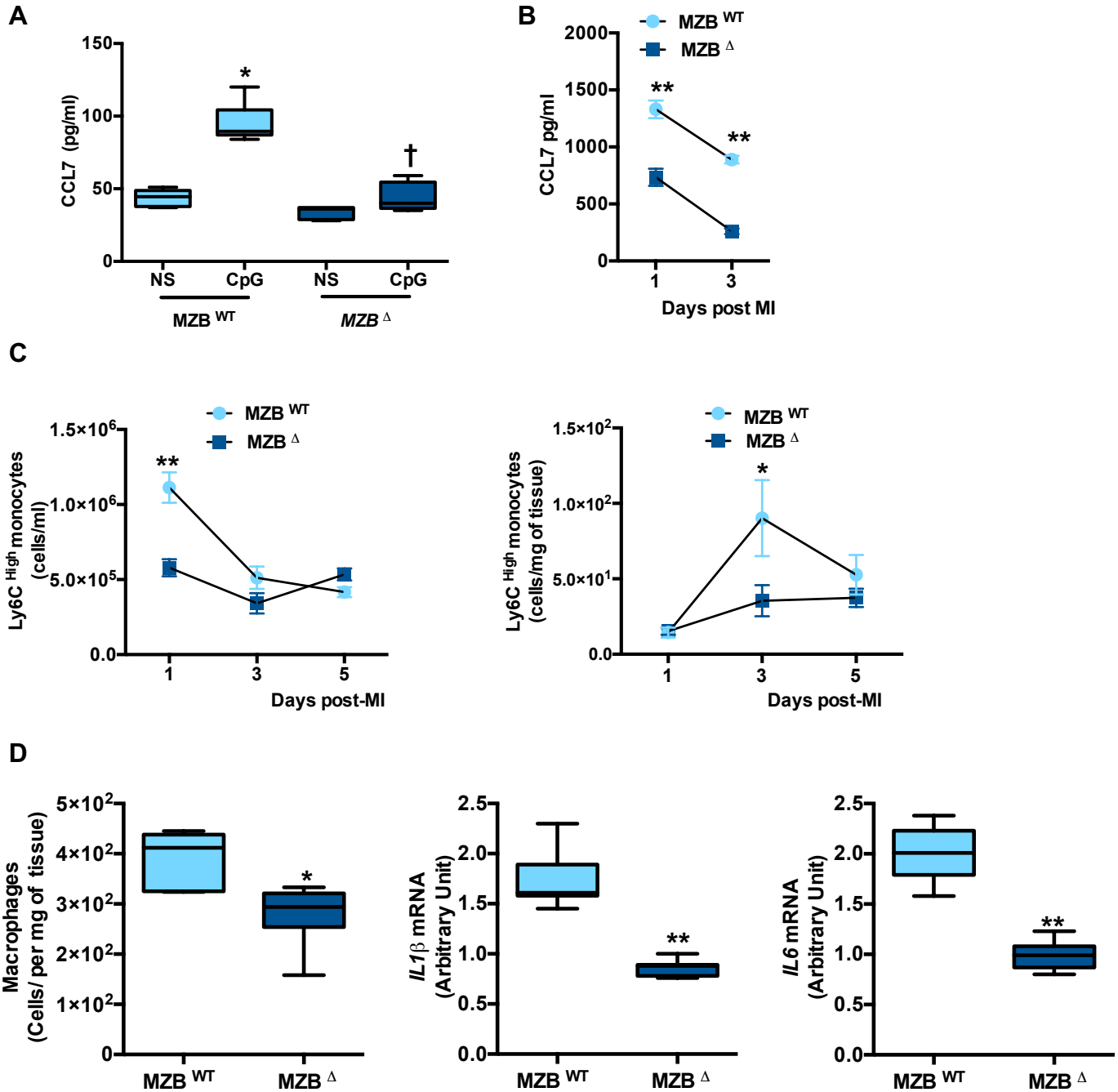
A
CCL7 (pg/ml)
150
100
50
0
*
†
NS
CpG
NS
CpG
MZB WT
MZB Δ
B
MZB WT
MZB Δ
CCL7 pg/ml
2000
1500
1000
500
0
**
**
1
3
Days post MI
C
MZB WT
MZB Δ
Ly6C High monocytes (cells/ml)
1.5×10^6
1.0×10^6
5.0×10^5
0.0
**
1
3
5
Days post-MI
MZB WT
MZB Δ
Ly6C High monocytes (cells/mg of tissue)
1.5×10^2
1.0×10^2
5.0×10^1
0.0
*
1
3
5
Days post-MI
D
Macrophages (Cells/ per mg of tissue)
5×10^2
4×10^2
3×10^2
2×10^2
1×10^2
0
*
MZB WT
MZB Δ
IL1β mRNA (Arbitrary Unit)
2.5
2.0
1.5
1.0
0.5
0.0
**
MZB WT
MZB Δ
IL6 mRNA (Arbitrary Unit)
2.5
2.0
1.5
1.0
0.5
0.0
**
MZB WT
MZB Δ

Figure 6

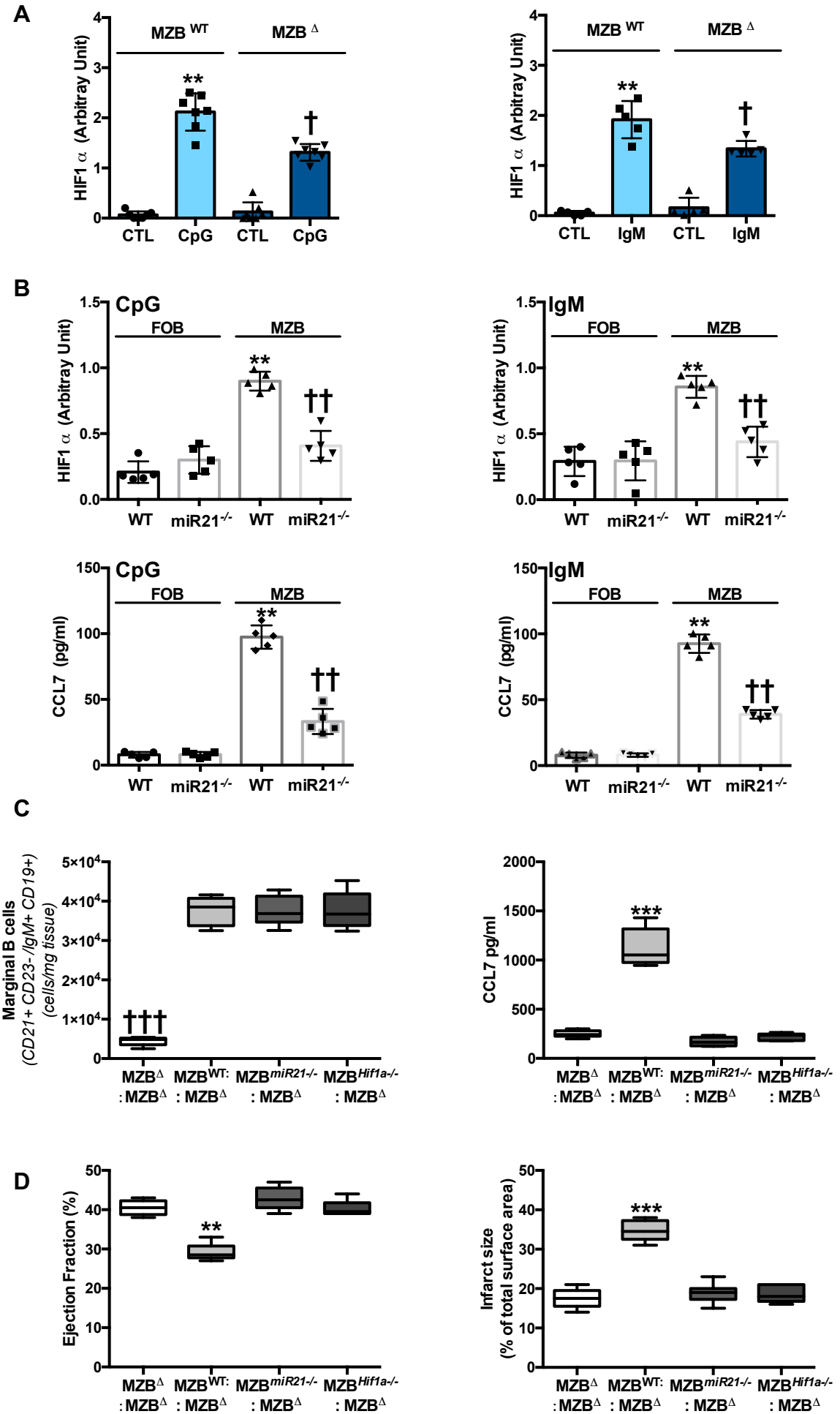
A
MZB WT
MZB Δ
HIF1 α (Arbitray Unit)
CTL
CpG
IgM
B
CpG
IgM
FOB
MZB
WT
miR21-/-
CCL7 (pg/ml)
C
Marginal B cells
(CD21+ CD23-/IgM+ CD19+)
(cells/mg tissue)
CCL7 pg/ml
MZBΔ :MZBΔ
MZBWT: :MZBΔ
MZBmiR21-/- :MZBΔ
MZBHif1a-/- :MZBΔ
D
Ejection Fraction (%)
Infarct size
(% of total surface area)

Figure 7

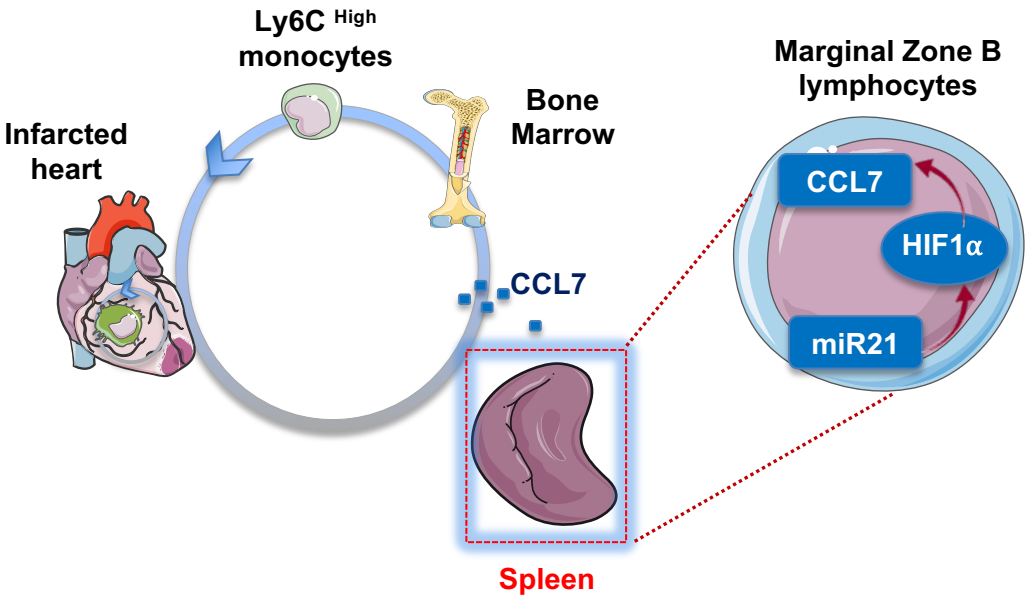


Central illustration

**Supplemental methods**

***Experimental procedures***

Male and female mice of 12 week-old were used. C57BL/6J and *Rag1*$^{-/-}$ mice were obtained from Janvier (France). For evaluation of the role of HIF-1α and HIF-2α in B cells: *Cd79a*$^{cre/+}$ mice were crossed with *Hif1a* $^{flox/flox}$ and/or *Hif2a* $^{flox/flox}$ animals to generate *Cd79a*$^{cre/+}$/*Hif1a* $^{flox/flox}$ (referred to as the *Hif1a*$^{-/-}$ B cell group); *Cd79a*$^{cre/+}$/*Hif2a* $^{flox/flox}$ (referred to as the *Hif2a*$^{-/-}$ B cell group); *Cd79a*$^{cre/+}$/*Hif1a-Hif2a* $^{flox/flox}$ (referred to as the *Hif1a-2a*$^{-/-}$ B cell group) mice and their littermates *Cd79a*$^{+/+}$/*Hif1a* $^{flox/flox}$, *Cd79a*$^{+/+}$/*Hif2a* $^{flox/flox}$ or *Cd79a*$^{+/+}$/*Hif1a- Hif2a* $^{flox/flox}$ (referred to as the WT B cell groups). For evaluation of the role of marginal zone B cells (MZB), *Cd79a*$^{cre/+}$ animals were crossed with *Rbpjk* $^{flox/flox}$ mice to generate *Cd79a*$^{cre/+}$/*Rbpjk* $^{flox/flox}$ (referred to as the MZB$^{\Delta}$ group lacking MZB cells) and *Cd79a*$^{+/+}$/*Rbpjk* $^{flox/flox}$ (referred to as the MZB$^{WT}$ group) animals.

***Myocardial infarction***

Myocardial infarction was induced by left coronary ligation, as previously described (1). Mice were anesthetized using Ketamine (100 mg/kg body weight) and Xylazine (10 mg/kg body weight) via intra-peritoneal injection, intubated and ventilated using a small-animal respirator. The chest wall was shaved and a thoracotomy was performed in the fourth left intercostal space. The pericardial sac was removed, and the left anterior descending artery was permanently ligated using a 7/0 monofilament suture (Peters surgical, France) at the site of its emergence close to the left atrium. The thoracotomy was closed with 6/0 monofilament sutures. The exact same procedure was performed for the sham-operated mice except that the ligation was not tied. The endotracheal tube was removed once spontaneous respiration was resumed, and mice were placed on a warm pad at 37 °C until awakened. In a second set of experiment, anesthetized mice

were mechanically ventilated, and ischemia was produced by occluding the left coronary artery with a 7/0 monofilament suture (Peters surgical, France) on a tapered BV-1 needle for 40 minutes. Following 40 minutes of occlusion, the ligature was released. All experiments were performed with 10 to 25-week-old male animals and were carried out using age and littermate matched groups without randomization.

***Chimeric mice***

To evaluate the role of miR21, bone marrow cells were obtained by flushing tibiae and femora of donor mice. Wild-type mice were lethally irradiated with a total dose of 9.5 Gy and were intravenously injected 24 hours later with $1x10^7$ total bone marrow cells from *miR21*$^{-/-}$ or their wild-type littermates. Mice were then challenged with MI 8 weeks after bone-marrow reconstitution, as previously described (2). To assess the role of B lymphocyte expressing miR21, 7 days before MI induction, *Rag1*$^{-/-}$mice received either 2 x $10^7$ wild-type splenocytes, 1.2 x $10^7$ B cell-depleted splenocytes recovered from CD20 monoclonal antibody treated mice (200µg/mouse), as previously described (1), B cell-depleted splenocytes re-supplemented with 8 x $10^6$ wild-type B lymphocytes or with 8 x $10^6$ *miR21*$^{-/-}$ B lymphocytes.

For evaluation of the role of miR21 and HIF-1α in MZB cells, *Cd79a*$^{cre/+}$/*Rbpjk*$^{flox/flox}$ recipient mice deficient for marginal zone B cells were partially irradiated with a total dose of 4.0 Gy and injected with $5x10^6$ total bone marrow cells isolated from *Cd79a*$^{+/+}$/*Rbpjk*$^{flox/flox}$ (referred to as the MZB$^{WT}$:MZB$^{\Delta}$ group), *Cd79a*$^{cre/+}$/*Rbpjk*$^{flox/flox}$ (referred to as the MZB$^{\Delta}$:MZB$^{\Delta}$ group), *miR21*$^{-/-}$ (referred to as the MZB$^{miR21-/-}$:MZB$^{\Delta}$ group) or *Cd79a*$^{cre/+}$/*Hif1a*$^{flox/flox}$ (referred to as MZB$^{Hif1a-/-}$:MZB$^{\Delta}$ group) animals, as previously described (3). Mice were then challenged with MI after 6 weeks.

***Echocardiographic measurements***

Transthoracic echocardiography was performed 14 days after surgery using an echocardiograph (ACUSON S3000 ultrasound, Siemens AG, Erlangen, Germany) equipped with a 14-MHz linear transducer (1415SP). The investigator was blinded to group assignment. Mice were anesthetized by isoflurane inhalation. Percentages of ejection fraction (%EF) were calculated, as previously described (4).

***Immunohistochemistry***

For evaluation of cardiac remodeling, hearts were excised, rinsed in PBS and frozen in liquid nitrogen. Hearts were cut by a cryostat (CM 3050S, Leica) into 5-7µm thick sections. Masson's trichrome and Sirius red stains were performed for infarct size and myocardial fibrosis evaluation, respectively. Infarct size was calculated as the ratio of total infarct circumference divided by total left ventricle circumference. The collagen volume fraction was calculated as the ratio of the total area of interstitial fibrosis to the myocyte area in the entire visual field of the section. Endothelial cells within capillaries were visualized after Bandeiraea Simplicifolia lectin staining (1:100, FITC-conjugated Griffonia simplicifolia, Sigma-Aldrich), and cardiomyocytes after Wheat Germ Agglutinin staining (1:200, Texas Red-conjugated, ThermoFisher).

***Flow cytometry***

Left ventricles and spleens were isolated, minced with fine scissors and gently passed through the Bel-Art™ Scienceware™ 12-Well Tissue Disaggregator (Fisher Scientific). Cells were collected, filtered through 40µm nylon mesh and washed with PBS with 1%v/v Fetal Bovine Serum. Red blood cells were removed by incubation in hemolysis buffer (StemCell

Technologies). Cells were counted and used for FACS sorting or analyser, as previously described (4).

Single-cell suspensions of spleen, blood and heart were stained with fluorophore-conjugated antibodies in phosphate buffered saline at 4°C. Total cells were gated on Alexa Fluor 700-conjugated CD45 (30-F11, BD Biosciences) and the following antibodies were used: Pe-Cy7-conjugated anti-CD11b (M1/70, BD Pharmingen), phycoerythrin-conjugated anti-Ly6G (1A8, BD Pharmingen), FITC–conjugated anti-Ly6C (AL-21, BD Pharmingen), APC-conjugated anti-IgM (II-41, ebiosciences) PE-conjugated anti-CD23 (B3/B4, ebiosciences), FITC-conjugated anti-CD21 (eBio4E3, ebiosciences), BV421-Conjugated anti-CD64 (X54-5/7.1, Biolegend), APC-conjugated anti-F4/80 (MCA497, AbD Serotec, Bio-Rad), Pe-Cy7-conjugated anti-CD19 (1D3, BD). All antibodies were used at a dilution of 1:100. The total number of cells was then normalized to tissue weight. Events were acquired on an X20 Fortessa flow cytometer (BD Biosciences) and results were analyzed on FlowJo software. Dead cells were excluded based on forward and side scatter profiles. B cells were identified as $IgM^{+}CD19^{+}$, MZB cells as $CD23^{lo/-}CD21^{hi}$, FOB cells as $CD23^{hi}CD21^{lo/-}$, monocytes were identified as $CD45^{+}CD11b^{+}F4/80^{-}Ly6G^{-}$ and $Ly6C^{High}$ or $^{Low}$ cells, macrophages as $CD45^{+}CD11b^{+}Ly6G^{-}F4/80^{+}CD64^{+}$ cells.

For MZB and FOB cell purification, B cell enriched populations were first separated by an autoMACS Pro Separator (Miltenyi Biotec) using a B cell purification kit (Miltenyi Biotec) according to the manufacturer's instructions. B cells were then stained for 15 min at 4 °C with anti-CD23-PE and anti-CD21-FITC. After washing and staining with 7-AAD to assess cell viability, MZB ($CD21^{hi}CD23^{lo}$) and FOB ($CD23^{hi}CD21^{lo}$) cells were sorted using a FACSAria II (BD Biosciences). The purity of both cell populations was higher than 95%.

***B lymphocyte isolation and culture***

MZB and FOB cells were isolated as described above and cultured in IMDM medium supplemented with 10% Fetal Bovine Serum, β-mercaptoethanol (Gibco), penicillin (100 U/ml), and streptomycin (100 µg/ml) and BAFF (20 ng/ml, R&D systems). Purified B cells ($1\times10^6$/500µl) were plated in 24-well cell culture plates and stimulated for 8 or 24 hours under the following conditions: CpG ODN1668 (1 µM, InvivoGen) or AffiniPure F(ab')$_2$ Fragment Goat anti-mouse IgM antibody (10 µg/ml, Jackson ImmunoResearch). Dimethyloxaloylglycine, (DMOG, 1mM, Sigma-Aldrich) was added in some conditions to inhibit HIFα degradation. HIF-1α transcriptional activity was measured using the HIF-1α transcriptional factor activity assay kit (ab133104, abcam) according to the manufacturer's instructions.

***Western Blot***

Cultured B cells were washed with ice-cold PBS and spun down. Cells were lyzed and proteins denatured by directly resuspending the pellet in 1X Laemmli Buffer (62,5 mmol/l Tris-HCl pH 6.8, 70mM SDS, 10% Glycerol, 1% 2-Mercaptoethanol). Proteins were separated on a freshly casted 9% Bis-Acrylamide gels and transferred onto nitrocellulose membranes (0.2µm Bio-Rad). After Ponceau red staining to evaluate transfer's efficiency and saturating non-specific binding sites with 3% Blotto (3% skimmed milk in TBS/0.05% Tween-20), HIF-1α (Novus, 100-449, 1:1000) and pan-actin (Chemicon international, MAB 1501, 1:1000) were blotted. In some cases, membranes were stripped with freshly prepared stripping buffer (2M Tris-HCL pH 6.8, 10% SDS, 100mM β-Mercaptoethanol) and re-probed. Blots were scanned before re-probing to assess stripping efficiency. ImageJ software (NIH) was used for immunoblots quantification.

***Quantitative real-time PCR***

Quantitative real-time PCR was performed on a Step One Plus (Applied Biosystems). The following primer sequences were used:

*GAPDH*: forward 5′-CGT-CCCGTAGACAAAATGGTGAA-3′, reverse 5′-GCCGTGAGTGGAGTCATACTGGAA-CA-3′; β-actin: forward 5’-GGT-CCA-CAC-CCG-CCA-CCA-GT-3’, reverse 5’-CGG-CCC-ACG-ATG-GAG-GGG-AAT-3’; *Hif1a* forward 5'-ACTGCACGGGCCATATTCATGTCT-3', reverse 5'-CTTCCGGCTCATAACCCATCAACT-3'; *Hif2a* forward 5'-CCGCCACAGTGCTATGCCTCCCAGTT-3', reverse 5'-CTTCCGGCTCATAACCCATCAACT-3'; *Il1ß*: forward 5'-GAAGAGCCCATCCTCTGTGA-3', reverse 5'-GGGTGTGCCGTCTTTCATTA-3'; *Il6*: forward 5'-AAGACAAAGCCAGAGTCCTTCAGAGAGA-3', reverse 5'-TAGCCACTCCTTCTGTGACTCCAGCTTA-3'; *Ccl7* forward: 5'-CCTGCTGCTCATAGCCGCTGCTTTC -3', reverse : 5'-AGCGCAGACTTCCATGCCCTTCTT -3'; *Col1a1*: forward 5’-TGCCCTCCTGACGCATGGCCAAGA-3’, reverse 5’-CCTCGGGTTTCCACGTCTCACCATT-3’; *Col3a1*: forward 5’-CACCCCGAACTCAACAGTGGAGAA-3’, reverse : 5’-ATGGGGCTGGCATTTATGCATGTT-3’; miR21 levels were quantified using real time qPCR TaqMan assay (Tm 00397, Applied Biosystems) following the manufacturer's instructions. miR21 expression was normalized to U6 snRNA (Tm 001973, Applied Biosystems) and snoRNA234 (Tm001234; Applied Biosystems) as ubiquitous controls. Relative expression was calculated using the 2-delta-delta CT method and expressed as arbitrary unit, as previously described (5).

***Chemokines levels***

Plasma levels of CCL7 were measured using Quantikine Elisa Kits (R&D Systems) according to the manufacturer's instructions.

***Statistical analysis***

Mice dying within 24 hours of coronary artery ligation surgery (<10% in all genotypes studied) were pre-specified as purely technical failures and excluded from subsequent analysis.

**Supplemental results**

To specifically substantiate the role of B cell expressing miR21, we injected B cell deficient *Rag1*$^{-/-}$ mice either with wild-type splenocytes, B cell depleted splenocytes, or B cell depleted splenocytes re-supplemented with wild-type or *miR21*$^{-/-}$ B lymphocytes. We first verified that re-supplementation with wild-type or *miR21*$^{-/-}$ B lymphocytes restored B cell numbers in spleens of *Rag1*$^{-/-}$ mice compared to mice injected with B cell-depleted splenocytes (Supplemental Figure 1B). Of interest, transfer of B cell-depleted splenocytes into *Rag1*$^{-/-}$ mice improved left ventricular ejection fraction after MI compared to the transfer of non-depleted splenocytes (Supplemental Figure 1C). This effect was abrogated after re-supplementation of B cell-depleted splenocytes with B lymphocytes isolated from WT mice but not with *miR21*$^{-/-}$ B lymphocytes (Supplemental Figure 1C). B cell depletion also reduced infarct size and interstitial fibrosis, which was antagonized by re-supplementation with WT but not *miR21*$^{-/-}$ B lymphocytes (Supplemental Figure 1D). Similarly, re-supplementation with WT B lymphocytes was associated with an increase of CCL7 levels compared to mice receiving B cell-depleted splenocytes. In contrast, re-supplementation of B cell-depleted splenocytes with B lymphocytes isolated from *miR21*$^{-/-}$ mice failed to increase CCL7 levels (Supplemental Figure 1E). Re-supplementation with WT B lymphocytes increased Ly6C$^{High}$ monocyte numbers in the blood and within the infarcted heart compared to administration of B cell-depleted splenocytes (Supplemental Figure 1F), a phenotype that was abrogated in mice re-supplemented with *miR21*$^{-/-}$ B lymphocytes (Supplemental Figure 1F).

**Supplemental Figures**

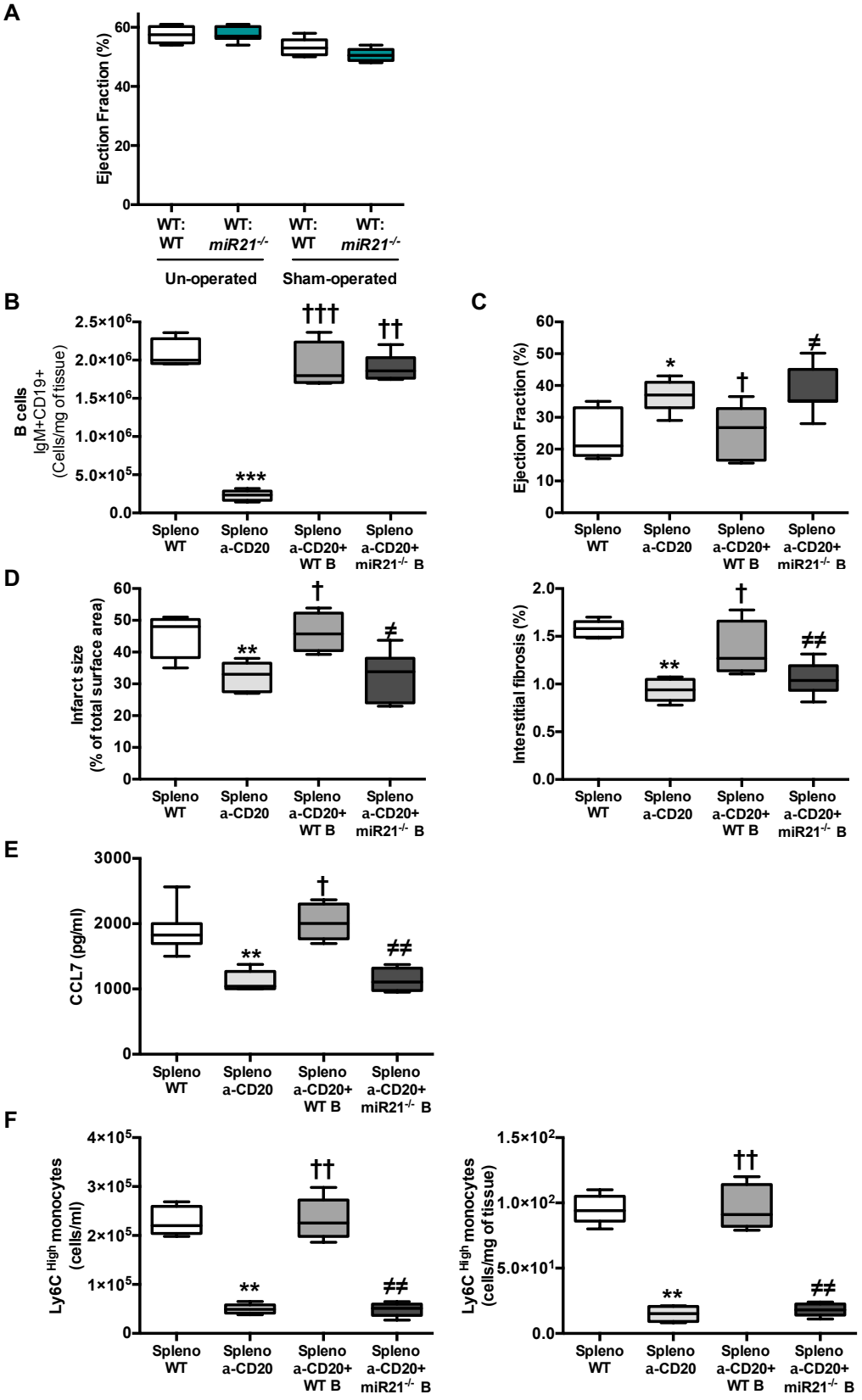


**Supplemental Figure 1**

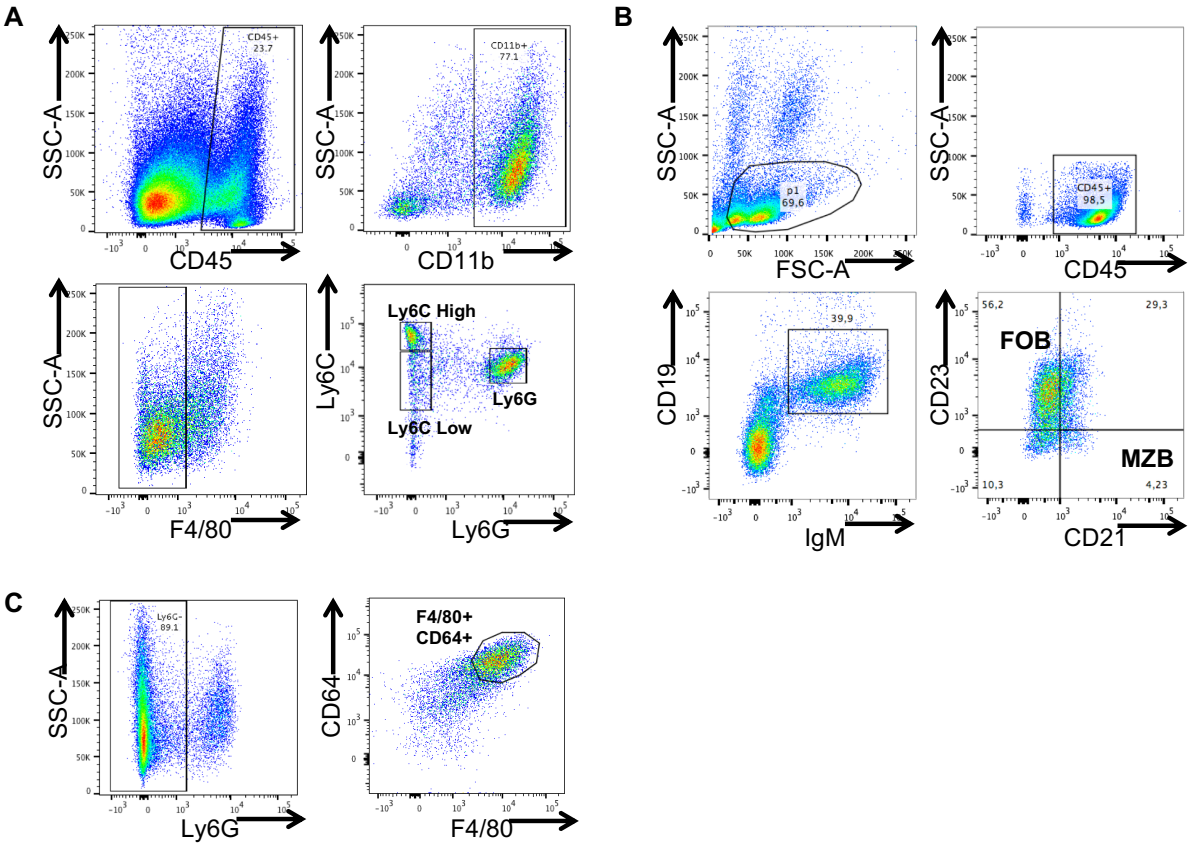


**Supplemental Figure 2**

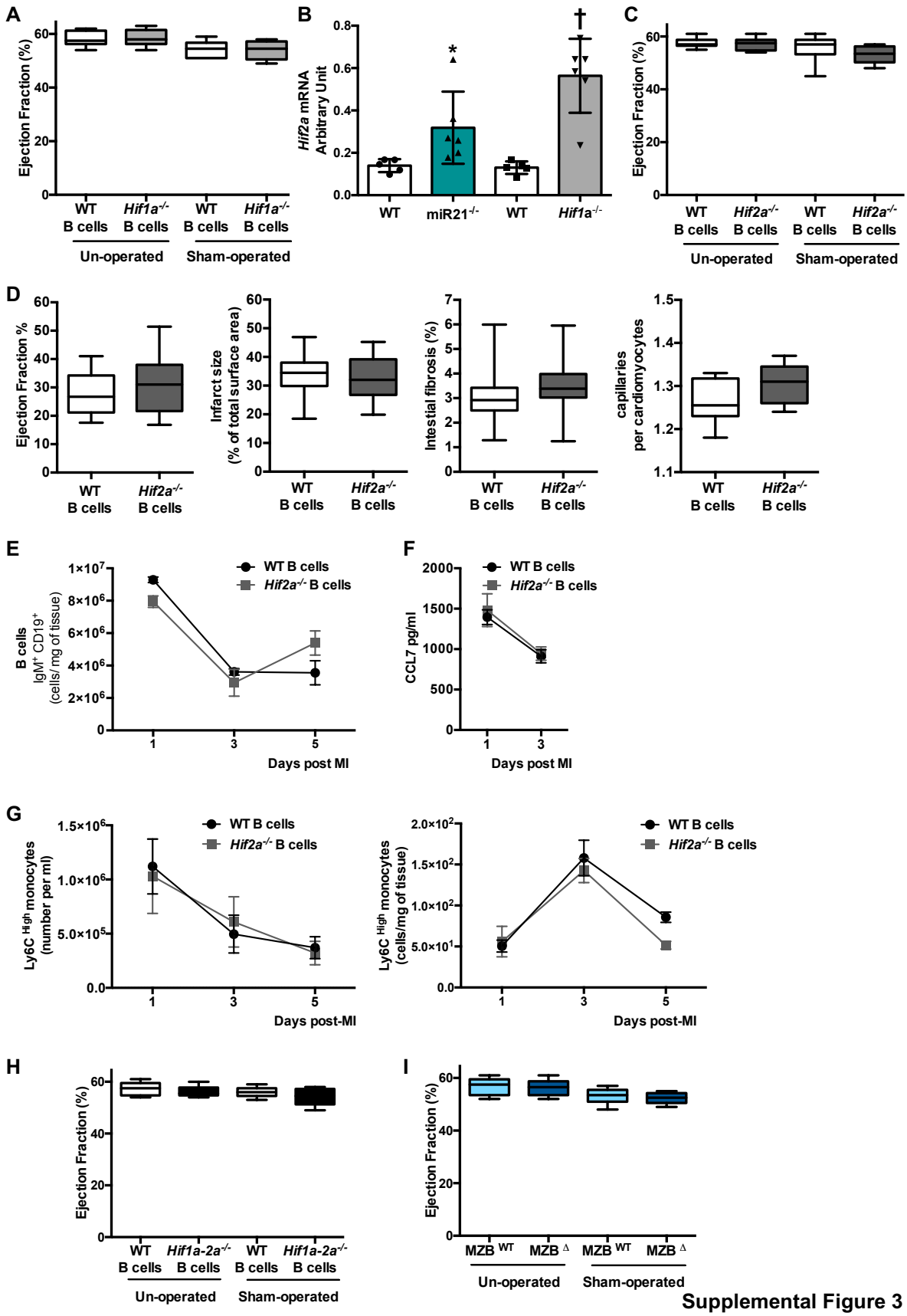


**Supplemental Figure 3**

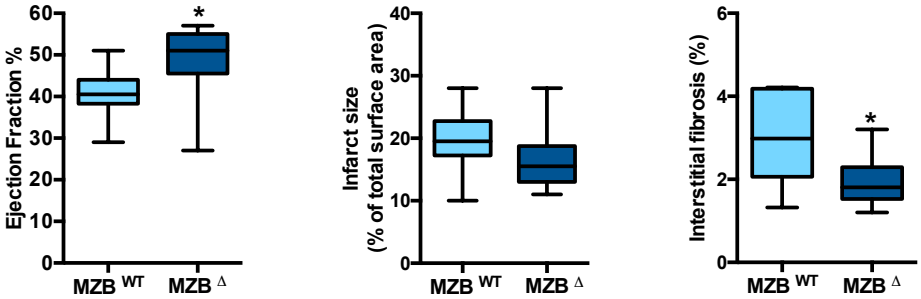


**Supplemental Figure 4**

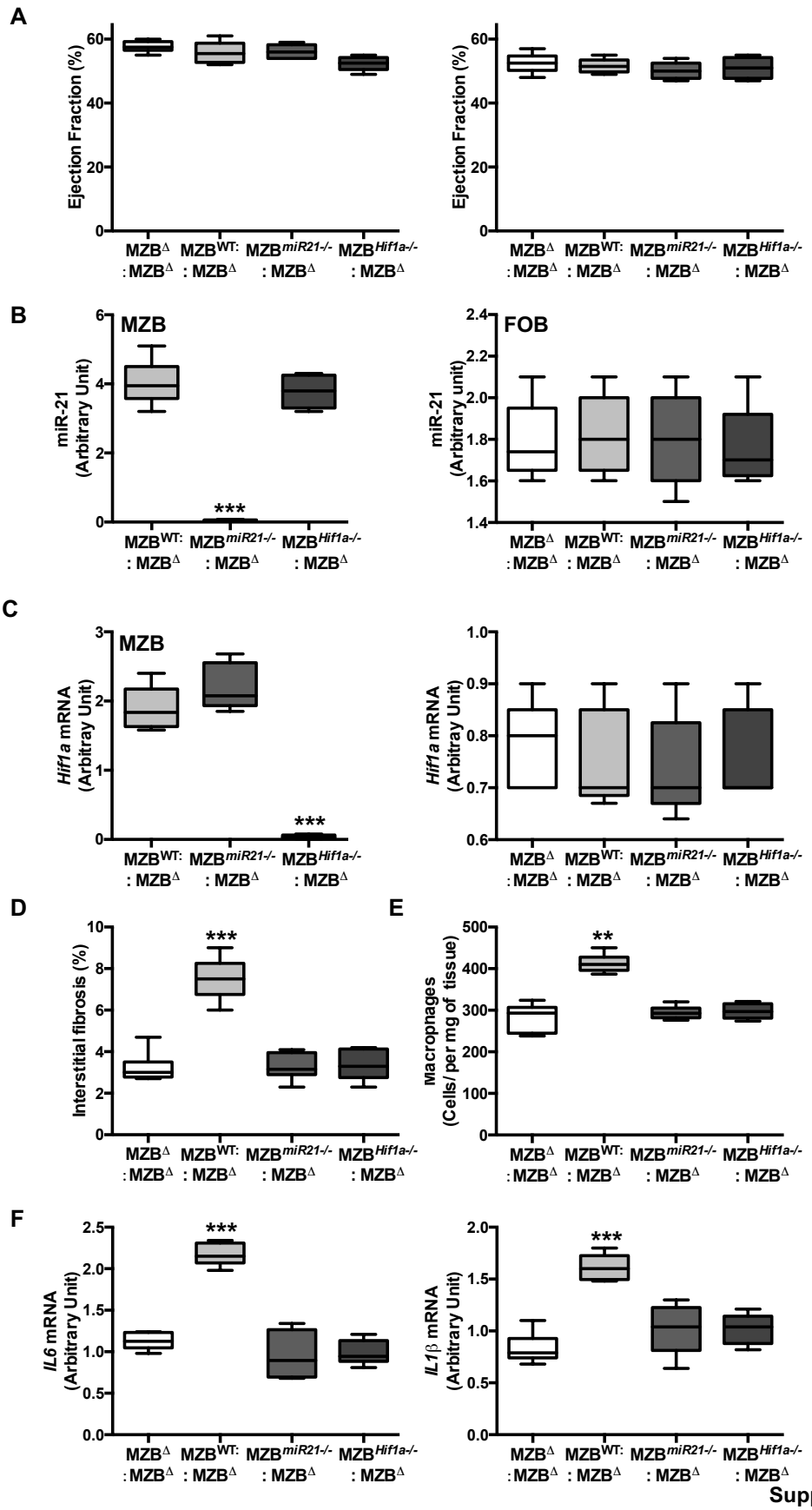


**Supplemental Figure 5**

**Supplemental Figure legends**

**Supplemental Figure 1**: **B cell expressing miR21 promote adverse ventricular remodeling after myocardial infarction.**

**A)** Left ventricle ejection fraction in un-operated and sham-operated (day 14 after the surgery) in WT:WT and WT:*miR21*$^{-/-}$ animals (n=5). **B)** Re-supplementation with WT and miR21-deficient B cells restored splenic B cell number (n=7, ***P<0.001 versus Spleno WT; ††P<0.01, †††P<0.001 versus Spleno a-CD20). **C-F)** miR21 deficiency in B cells improved ejection fraction (C), reduced infarct size (D, left), interstitial fibrosis (D, right), circulating CCL7 levels (E), Ly6C$^{High}$ monocytes number in the blood (F, left) and cardiac tissue (F, right). (n=7, *P<0.05, **P<0.01 versus WT splenocytes; †P<0.05, ††P<0.01 versus Spleno a-CD20 ; ≠P<0.05, ≠≠P<0.01 versus Spleno a-CD20+WT B). *Abbreviations :* Spleno WT indicates *Rag1*$^{-/-}$ mice injected with wild-type splenocytes; Spleno a-CD20: *Rag1*$^{-/-}$ mice injected with B cell-depleted splenocytes; Spleno a-CD20+WT B: *Rag1*$^{-/-}$ mice injected with B cell-depleted splenocytes re-supplemented with wild-type; Spleno a-CD20+miR21$^{-/-}$: *Rag1*$^{-/-}$ mice injected with B cell-depleted splenocytes re-supplemented with *miR21*$^{-/-}$ B cells. a-CD20 indicates that B cell-depleted splenocytes were recovered from CD20 monoclonal antibody treated mice. WT:WT or WT:*miR21*$^{-/-}$ lethally irradiated WT mice transplanted with bone marrow derived cells isolated from WT mice or miR21$^{-/-}$ animals, respectively.

**Supplemental Figure 2**: **Gating strategy for FACS analysis**.

**A)** Gating strategy for evaluation of monocyte subpopulations. Circulating or cardiac CD45$^{+}$/CD11b$^{+}$/F4/80$^{-}$ leukocytes were stratified by Ly6G and Ly6C expression. **B)** Gating strategy for evaluation of B subpopulations. Single cell tissue suspensions were prepared and labeled. Size (FSC-A) and granularity (SSC-A) was assessed by flow cytometry and CD45+

leukocytes were identified, gated on CD19 and IgM and then further stratified by CD23 and CD21 expression. FOB cells were identified as $CD23^{High}$ $CD21^{Low/-}$ and FOB cells as $CD23^{Low/-}$ and $CD21^{High}$. **B)** Gating strategy for evaluation of macrophage content. Cardiac $CD45^{+}/CD11b^{+}/Ly6G^{-}$ cells were identified as $F4/80^{+}/CD64^{+}$ macrophages. *Abbreviations :* FOB indicates follicular B cells; MZB, marginal zone B cells.

**Supplemental Figure 3: *Hif2a* deficiency in B cells does not modulate cardiac function.**

**A)** Left ventricle ejection fraction in un-operated and sham-operated (day 14 after the surgery) in *Hif1a*$^{-/-}$ B cells and WT B cells group. (n=5). **B)** *Hif2a* mRNA levels were increased in B cells isolated from *miR21*$^{-/-}$ mice and *Hif1a*$^{-/-}$ B cells group, at day 1 after MI (n=7, *P<0.05 for B cells isolated from infarcted WT mice, †P<0.05 versus B cells derived from infarcted WT B cells group). **C)** Left ventricle ejection fraction in un-operated and sham-operated (day 14 after the surgery) *Hif2a*$^{-/-}$ B cells and WT B cells group (n=5). **D-G)** Specific deletion of *Hif2a* in B cells did not impact cardiac function and remodeling (D), splenic B cell number (D), blood CCL7 levels (F), blood (G, left) and cardiac $Ly6C^{High}$ monocytes (G, right) (n=7). **H)** Left ventricle ejection fraction in un-operated and sham-operated (day 14 after the surgery) in *Hif1a-2a*$^{-/-}$ B cells and WT B cells group. (n=5). **I)** Left ventricle ejection fraction in un-operated and sham-operated (day 14 after the surgery) in $MZB^{WT}$ and $MZB^{\Delta}$ mice (n=6). *Abbreviations :* *Hif1a*$^{-/-}$ B cells, indicates mice with conditional deletion of *Hif1a* in B cells; *Hif2a*$^{-/-}$ B cells, mice with conditional deletion of *Hif2a* in B cells; *Hif1a-2a*$^{-/-}$ B cells mice with conditional deletion of *Hif1a* and *Hif2a* in B cells; and WT B cells, their wild-type littermates; MI myocardial infarction; $MZB^{\Delta}$ mice with conditional deletion of MZB cells and $MZB^{WT}$, their wild-type littermates.

**Supplemental Figure 4: MZB cell deficiency prevents myocardial-reperfusion injury.**

MZB cell deficiency improved ejection fraction and reduced interstitial fibrosis in experimental model of ischemia-reperfusion (n=12, *P<0.05), 14 days after the onset of reperfusion. *Abbreviations :* $MZB^{\Delta}$ indicates mice with conditional deletion of MZB cells and $MZB^{WT}$, their wild-type littermates.

**Supplemental Figure 5: miR21-HIF1α signaling shapes the deleterious effect of MZB cells.**

**A)** Left ventricle ejection fraction in un-operated (Left) and sham-operated (Right, day 14 after the surgery) in the different experimental groups (n=7). **B-C)** The experimental model was validated by the observation that miR21 contents were reduced in MZB cells of $MZB^{miR21-/-}$:$MZB^{\Delta}$ group (B) and that *Hif1a* mRNA levels were decreased in MZB cells of $MZB^{miR21-/-}$:$MZB^{\Delta}$ group. In addition, miR21 and *Hif1a* mRNA levels were unaffected in FOB cells whatever the experimental groups (n=5, ***P<0.01 versus the other groups). **D-F**) Specific deletion of *miR21* and *Hif1a* in MZB cells reduced interstitial fibrosis (D), cardiac macrophage number (E), cardiac *Il6* (F, left) and *Il1β* mRNA levels (n=5, *P<0.01, **P<0.001 for $MZB^{WT}$:$MZB^{\Delta}$ group versus other groups). *Abbreviations :* FOB indicates follicular B cells; MZB, marginal zone B cells. $MZB^{\Delta}$:$MZB^{\Delta}$, partially irradiated marginal zone B cell deficient mice ($MZB^{\Delta}$) retransplanted with bone marrow cells isolated from $MZB^{\Delta}$ mice; $MZB^{WT}$:$MZB^{\Delta}$, partially irradiated $MZB^{\Delta}$ mice retransplanted with bone marrow cells isolated from $MZB^{WT}$ mice; $MZB^{miR21-/-}$:$MZB^{\Delta}$, partially irradiated $MZB^{\Delta}$ mice retransplanted with bone marrow cells isolated from miR21 deficient mice; $MZB^{Hif1a-/-}$:$MZB^{\Delta}$, partially irradiated $MZB^{\Delta}$ mice retransplanted with bone marrow cells isolated from mice with $Hif1a^{-/-}$ B cells.

**Supplemental References**


1. Zouggari Y, Ait-Oufella H, Bonnin P et al. B lymphocytes trigger monocyte mobilization and impair heart function after acute myocardial infarction. Nature medicine 2013;19:1273-80.
2. Howangyin KY, Zlatanova I, Pinto C et al. Myeloid-Epithelial-Reproductive Receptor Tyrosine Kinase and Milk Fat Globule Epidermal Growth Factor 8 Coordinately Improve Remodeling After Myocardial Infarction via Local Delivery of Vascular Endothelial Growth Factor. Circulation 2016;133:826-39.
3. Nus M, Basatemur G, Galan M et al. NR4A1 Deletion in Marginal Zone B Cells Exacerbates Atherosclerosis in Mice-Brief Report. Arteriosclerosis, thrombosis, and vascular biology 2020;40:2598-2604.
4. Ngkelo A, Richart A, Kirk JA et al. Mast cells regulate myofilament calcium sensitization and heart function after myocardial infarction. The Journal of experimental medicine 2016;213:1353-74.
5. Loyer X, Paradis V, Henique C et al. Liver microRNA-21 is overexpressed in non-alcoholic steatohepatitis and contributes to the disease in experimental models by inhibiting PPARalpha expression. Gut 2016;65:1882-1894.